TITLE

pop-1/TCF, *ref-2/ZIC* and T-box factors regulate the development of anterior cells in the *C. elegans* embryo

AUTHORS

Jonathan D. Rumley[1], Elicia A. Preston[1], Dylan Cook[1], Felicia L. Peng[1], Amanda L. Zacharias[2,3], Lucy Wu[1], Ilona Jileaeva[1], John Isaac Murray[1,4]

1. **Department of Genetics, Perelman School of Medicine, University of Pennsylvania, Philadelphia, PA 19104**
2. **Division of Developmental Biology, Cincinnati Children's Hospital Medical Center, Cincinnati, OH 45229**
3. **Department of Pediatrics, University of Cincinnati College of Medicine, Cincinnati, OH 45267**
4. **Corresponding author - jmurr@pennmedicine.upenn.edu**

ABSTRACT

Patterning of the anterior-posterior axis is fundamental to animal development. The Wnt pathway plays a major role in this process by activating the expression of posterior genes in animals from worms to humans. This observation raises the question of whether the Wnt pathway or other regulators control the expression of the many anterior-expressed genes. We found that the expression of five anterior-specific genes in *Caenorhabditis elegans* embryos depends on the Wnt pathway effectors *pop-1/TCF* and *sys-1/*β-catenin. We focused further on one of these anterior genes, *ref-2/ZIC,* a conserved transcription factor expressed in multiple anterior lineages. Live imaging of *ref-2* mutant embryos identified defects in cell division timing and position in anterior lineages. *Cis*-regulatory dissection identified three *ref-2* transcriptional enhancers, one of which is necessary and sufficient for anterior-specific expression. This enhancer is activated by the T-box transcription factors TBX-37 and TBX-38, and surprisingly, concatemerized TBX-37/38 binding sites are sufficient to drive anterior-biased expression alone, despite the broad expression of TBX-37 and TBX-38. Taken together, our results highlight the diverse mechanisms used to regulate anterior expression patterns in the embryo.

INTRODUCTION

Anterior-posterior patterning regulation

Proper anterior-posterior patterning is critical for animal embryonic development and requires the Wnt pathway across all bilaterian animals from worms to humans. Typically, posterior cell identities are induced by posteriorly-produced Wnt ligands signaling through the canonical Wnt pathway [1]. In this pathway, signal transduction in response to Wnt activates posterior-expressed gene transcription through the transcription factor TCF and its co-activator β-catenin [2]. Although this conserved role for the Wnt pathway in regulating the expression of posterior genes is well documented [3], much less is known about how genes expressed in anterior cells are regulated.

Caenorhabditis elegans has been widely used to study anterior-posterior patterning because it is genetically tractable, its embryonic lineage is invariant, and most of its developmental regulators are highly conserved in vertebrates and other animals [4–10]. Also, the majority of embryonic cell divisions are oriented along the anterior-posterior axis, and require the Wnt pathway to differentiate the two daughter fates [11–13]. Following each anterior-posterior cell division, the Wnt pathway is activated in the more posterior daughter cell, leading to high nuclear SYS-1/β-catenin and low nuclear POP-1/TCF, whereas the anterior daughter cell has low nuclear SYS-1 and high nuclear POP-1[11–13]. The combination of high nuclear SYS-1 and low nuclear POP-1 in posterior cells makes it stoichiometrically favorable for POP-1 to be bound to posterior-expressed targets as a complex with SYS-1, thereby driving their expression [14–16]. In contrast, anterior cells have low nuclear SYS-1 and high nuclear POP-1; for posterior-expressed targets, this results in POP-1 being bound in the absence of SYS-1, allowing it to recruit co-repressors, including UNC-37/groucho [17] (Fig 1A). Loss of POP-1/TCF results in posterior genes having either reduced expression in posterior cells or increased expression in anterior cells, indicative of its dual roles as an activator and repressor. Loss of SYS-1/β-catenin results only in down-regulation of posterior genes in posterior cells, consistent with an exclusive role as a posterior activator [13]. These observations leave open the question of how anterior genes are regulated in *C. elegans*.

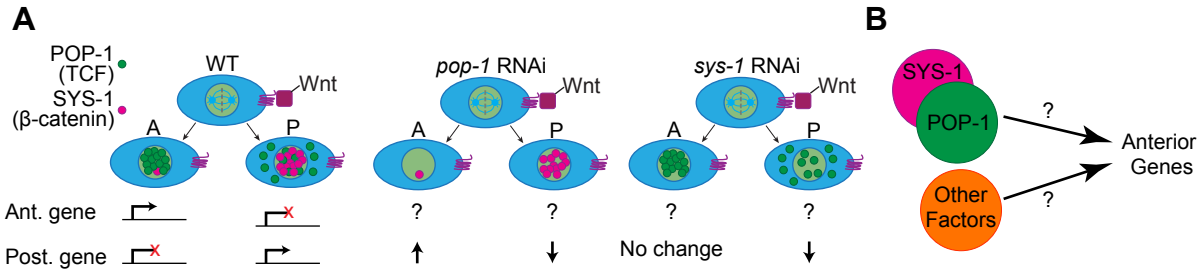

Fig 1. How are anterior genes regulated?
(A) The Wnt/β-catenin asymmetry pathway regulates anterior-posterior patterning by producing asymmetric nuclear concentrations of POP-1/TCF and SYS-1/β-catenin in anterior and posterior sister cells. Low nuclear concentrations of POP-1 and high nuclear concentrations of SYS-1 in the posterior cell activate expression of posterior genes and are associated with the lack of expression of anterior genes. Conversely, high nuclear concentrations of POP-1 and low nuclear concentrations of SYS-1 in the anterior cell repress posterior genes and are associated with expression of anterior genes. Effects of *pop-1* and *sys-1* RNAi on posterior genes are shown; effects on most anterior genes are unknown. (B) In this work, we test whether *pop-1*/TCF and *sys-1*/β-catenin regulate anterior genes in the *C. elegans* embryo, and ask what other factors also regulate anterior expression.

Previous work suggests at least three possible mechanisms by which anterior genes could be regulated. 1) They may be regulated by the Wnt pathway indirectly, with posteriorly-expressed canonical Wnt targets repressing the expression of anterior genes in posterior cells. 2) They may be directly regulated by Wnt pathway components acting in a modified (or "opposite") manner. 3) They may be regulated by a non-Wnt-related mechanism (Fig 1B).

An example of indirect Wnt pathway regulation through a posterior repressor is seen in the *C. elegans* embryonic EMS lineage, in which cells derived from the posterior daughter of EMS, E, express the POP-1-activated, gut-specifying transcription factor *end-1*. In turn, *end-1* represses the transcription factor *ceh-51*, which is normally expressed in and specifies the lineage derived from the anterior daughter of EMS, MS [18,19].

Conversely, the *C. elegans* anterior gene *ttx-3* is directly regulated by Wnt pathway components. *ttx-3* helps specify the AIY neuron class and is regulated by POP-1 and SYS-1 in a manner dependent on the sole *C. elegans* ZIC family transcription factor REF-2 [20]. After the AIY grandmother divides, *ttx-3* is expressed in the anterior daughter, the AIY mother, but not in the posterior daughter. In the AIY mother, the Wnt pathway is inactive, with low nuclear SYS-1 and

high nuclear POP-1, and both *pop-1* and *ref-2* are required to activate *ttx-3* expresion. In its posterior sister, the Wnt pathway is active, with high nuclear SYS-1 levels and low nuclear POP-1 levels, and *sys-1* is required to repress expression of *ttx-3*. Furthermore, POP-1 and REF-2 can directly interact, suggesting that REF-2 and POP-1 bind as a complex to activate *ttx-3* expression in the AIY mother. The role of SYS-1 is less clear but some evidence suggests SYS-1 may bind to the POP-1/REF-2 complex to repress expression, or may sequester away the limited POP-1, such that POP-1 cannot interact with REF-2 [20,21]. Similar regulation, termed "opposite Wnt regulation", has also been seen in other organisms such as *Drosophila* [22].

Because of the role of POP-1 and SYS-1 in regulating the anterior-specific expression of *ttx-3*, we hypothesized that these genes may also regulate other anterior genes. POP-1 and SYS-1 could act as general anterior expression regulators, interacting with lineage-restricted co-regulators to ensure appropriate expression of anterior genes in the correct lineages [20,21]. We tested this by mining single-cell-resolution expression data to identify transcription factors expressed in anterior-specific patterns, and show that of five we tested, all require *pop-1* and/or *sys-1* for either anterior expression or posterior repression. We focus in more detail on a single anterior-specific gene, *ref-2/ZIC*. By automated lineage analysis of mutants we find that *ref-2* is required for normal cell division timing and cell position in *ref-2* expressing lineages. Embryonic expression of *ref-2* is driven by at least three developmental enhancers, two of which drive early embryonic expression and one of which drives expression in later-stage embryos. The most distal enhancer (3.9 kb upstream of the transcription start site) drives highly anterior-biased expression. Functional dissection revealed unexpected redundancy within this enhancer, and a role for the T-box transcription factors *tbx-37* and *tbx-38* in driving anterior-specific expression. Surprisingly, concatemers of a single T-box binding site reiterate much of the anterior-specific expression pattern of *ref-2* in early embryos, suggesting a key role for these genes in driving anterior expression.

RESULTS

Many early embryonic transcription factors have anterior-specific expression

We used large-scale single-cell expression databases derived from time-lapse 4D imaging of embryos expressing reporter genes to identify anterior-expressed genes (Fig 2A). We define "anterior" or "posterior" lineages as sets of related cells derived from either the more-anterior or more-posterior daughter after a specific cell division (Fig 2B). Notably, this is distinct from physical position; for example, a cell that divides near the posterior pole of the embryo gives rise to both an anterior and posterior daughter lineage, both of which are located in the posterior half of the embryo (Fig 2B, left side). Following convention [5,23], all lineage trees in this manuscript are drawn with the more anterior daughters on the left and the posterior daughters on the right of each bifurcation. Earlier studies identified a strong tendency for genes to be expressed in either multiple anterior or multiple posterior lineages during early and mid-embryogenesis; these frequently appear as "lineally repetitive" patterns, with multiple related anterior or posterior cousin lineages all expressing the same gene (e.g. *nob-1* and *ref-2* in Fig 2D,E) [24,25]. Both anterior-specific and posterior-specific gene expression were similarly common. While posterior specific genes (e.g. Fig 2D) appear to be largely regulated by canonical Wnt signaling [13], it is less clear how anterior-specific patterns are regulated. We mined existing literature and large-scale databases of fluorescent reporter expression patterns (Fig 2A) [24–26] to identify 19 conserved genes expressed in anterior lineage-specific patterns (Fig 2C); the anterior-biased expression of these genes is also seen in embryonic single-cell RNA-seq data [27].

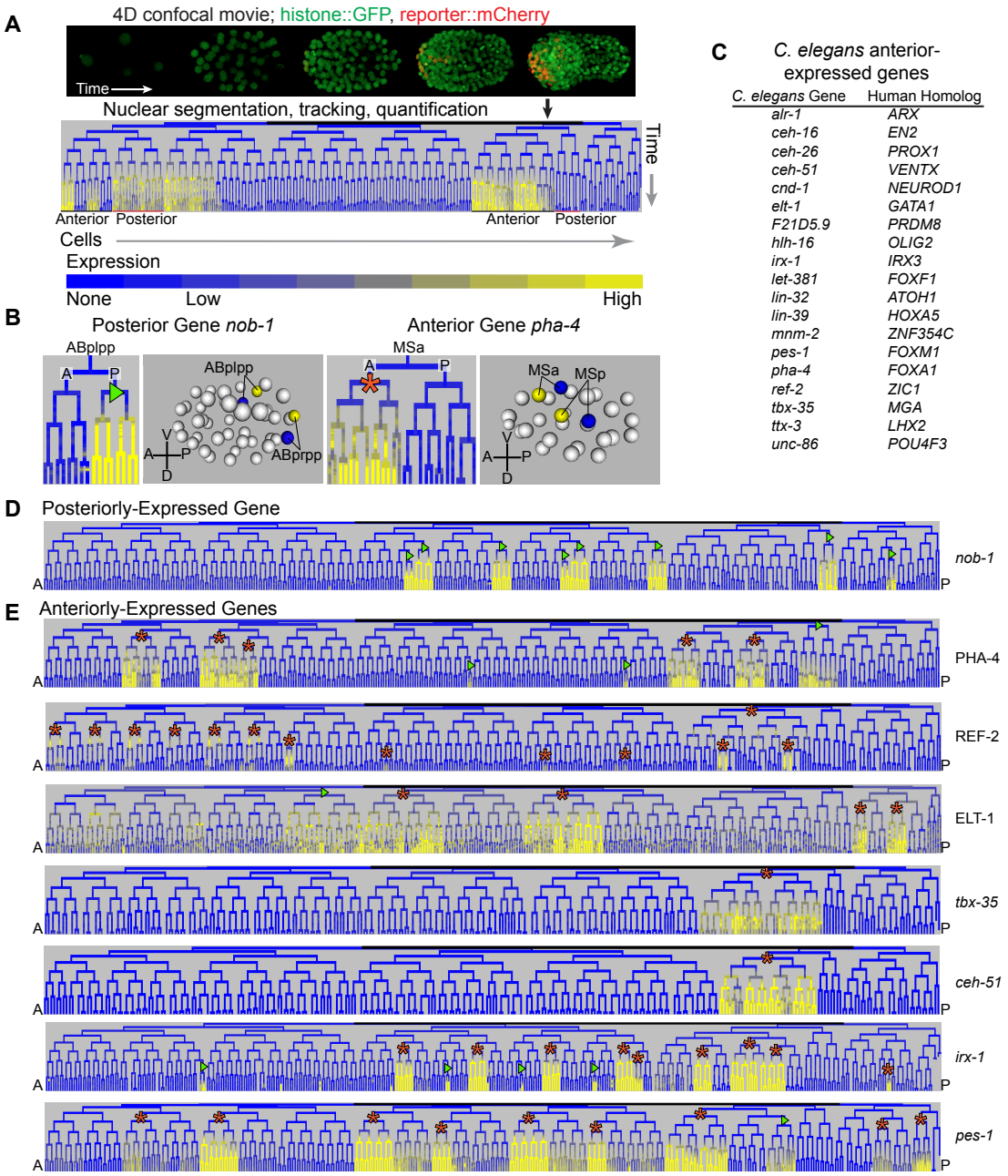

Fig 2. Identification of genes with anterior-biased expression.
(A) Automated lineaging traces lineages and quantifies expression from 4D confocal movies. In the lineage trees, vertical lines represent cells, and horizontal lines represent cell divisions. Most cells divide along the anterior-posterior axis, with anterior cells depicted on the left branch and posterior cells on the right branch. (B) Posterior and anterior genes are denoted as such based on their expression in cells descended from either a posterior or anterior sister cell, respectively, following an anterior-posterior cell division. Anterior and posterior genes can generally be expressed in cells from any part of the embryo. Anterior and posterior founder cells are labeled with orange asterisks/green triangles respectively. (C) List of anterior-biased genes in the EPiC database along with their predicted human homologs. (D) Expression pattern of a posterior gene, *nob-1/Hox9-13*. (E) Expression patterns of several anterior genes; most are expressed in unique combinations of mostly anterior lineages.

159 We confirmed the anterior-biased expression of seven of these by live confocal imaging followed
160 by automated cell tracking and lineage tracing (Fig 2A, E, Fig S1, Fig S2, Fig S3) [26,28]. For
161 each gene, we collected 3D timelapse movies of transgenic embryos expressing a histone-mCherry
162 (*pha-4*, *ref-2*, *elt-1*, *tbx-35*, *irx-1*, and *pes-1*), or GFP (*ceh-51*) reporter under the control of
163 upstream regulatory sequences of each gene (referred to here as "promoter reporters"). For five
164 genes we also collected images for fosmid transgenes (*irx-1, elt-1, pha-4* and *ref-2)* or CRISPR
165 knock-ins (*ceh-51*) in which the protein is fused to GFP and surrounded by its normal genomic
166 context ("protein reporters"). Each embryo also contained a ubiquitously expressed second-color,
167 histone-GFP or histone-mCherry fusion, used for cell tracking. We identified each nucleus at each
168 time point and traced them across time using StarryNite [28,29] cell tracking software, and used
169 AceTree [30,31] for subsequent manual error correction and validation that the extracted lineages
170 were correct. Finally, we quantified the expression of the reporter in each nucleus at each time
171 point (Fig 2A) [26]. The results confirm the anterior-specific expression of each gene, and, in some
172 cases, identify previously unknown expression patterns (Fig S1, Fig S2, Fig S3). For each promoter
173 reporter, the anterior-specific patterns were consistent, but the protein fusion reporters all had
174 additional expressing lineages and dynamics indicative of distal enhancers and post-transcriptional
175 regulation (Fig S1, Fig S2, Fig S3).
176
177 **The Wnt pathway effectors *pop-1* and *sys-1* are required for normal anterior-specific**
178 **expression**
179
180 Most genes expressed preferentially in posterior lineages require the Wnt effector transcription
181 factor POP-1/TCF either for activation in posterior cells (together with its coactivator SYS-1/β-
182 catenin) or for repression in anterior cells, and at least some are direct targets [12,13,32–35].
183 Although *pop-1* is required for the normal expression of some anterior genes [20,32,36], it is
184 unclear whether *pop-1* and *sys-1* are generally required for anterior-specific expression, as they
185 are for posterior-specific expression.
186
187 To test this, we measured the expression of five anterior gene reporters (*tbx-35*, *ceh-51*, *elt-1*, *irx-*
188 *1*, and *ref-2*) after *pop-1* and *sys-1* RNAi by live 3D imaging and lineage tracing as described
189 above. We used promoter reporters for *tbx-35*, *ceh-51*, *irx-1*, and *ref-2* because our wild-type

190 expression data indicated these reporters are sufficient for anterior regulation (Fig S1, Fig S2, Fig
191 S3). For *elt-1*, anterior-specific expression was more robust for the protein reporter so we tested
192 that reporter's dependence on *pop-1* and *sys-1* (Fig 3; Fig S4).
193
194 Reporters of two of the genes we tested, *tbx-35* and *ceh-51*, are expressed solely in the anterior
195 lineage MS (Fig S2; Fig S4A, B), and previous qualitative expression analyses indicated that
196 expression persists in the absence of *pop-1* [19,36,37]. Consistent with this, we detected expression
197 of both genes in the MS lineage after *pop-1* RNAi, however this expression was significantly
198 decreased. We also observed increased expression of both genes in the E lineage (posterior sister
199 of MS), although this expression remained lower than both the wild-type and *pop-1* RNAi MS
200 levels (Fig 3A, B; Fig S4A, B; Table S4). We also observe low-level ectopic expression of *tbx-35*
201 in the E lineage under *sys-1* RNAi. These results indicate that both *tbx-35* and *ceh-51* require *pop-*
202 *1* for full expression in the MS lineage and for repression in the E lineage (as shown previously
203 [19,36]), and that *sys-1* is required to repress *tbx-35* in the E lineage.
204
205 *elt-1* reporters are expressed in several early anterior lineages that primarily give rise to ectodermal
206 fates (ABpla, ABpra, Caa and Cpa), and in one posterior lineage (ABarp) (Fig S1; Fig S4C). In
207 the Caa and Cpa lineages, anterior lineages that express both the promoter and protein reporters,
208 *pop-1* RNAi results in decreased *elt-1* reporter expression. However, RNAi for neither *pop-1* nor
209 *sys-1* affects expression in their posterior sister lineages Cap and Cpp (Fig 3C; Fig S4C; Table S4).
210 Similarly, *pop-1* RNAi results in reduced expression of the protein reporter in the ABpla and
211 ABpra lineages, while RNAi knockdown of neither *pop-1* nor *sys-1* has much effect on their
212 posterior sister lineages ABplp and ABprp (Fig S4C; Table S4). Thus, in both the ABp and C
213 lineages, *pop-1* is required for anterior expression of *elt-1*, but neither *pop-1* nor *sys-1* is required
214 for posterior repression.
215
216

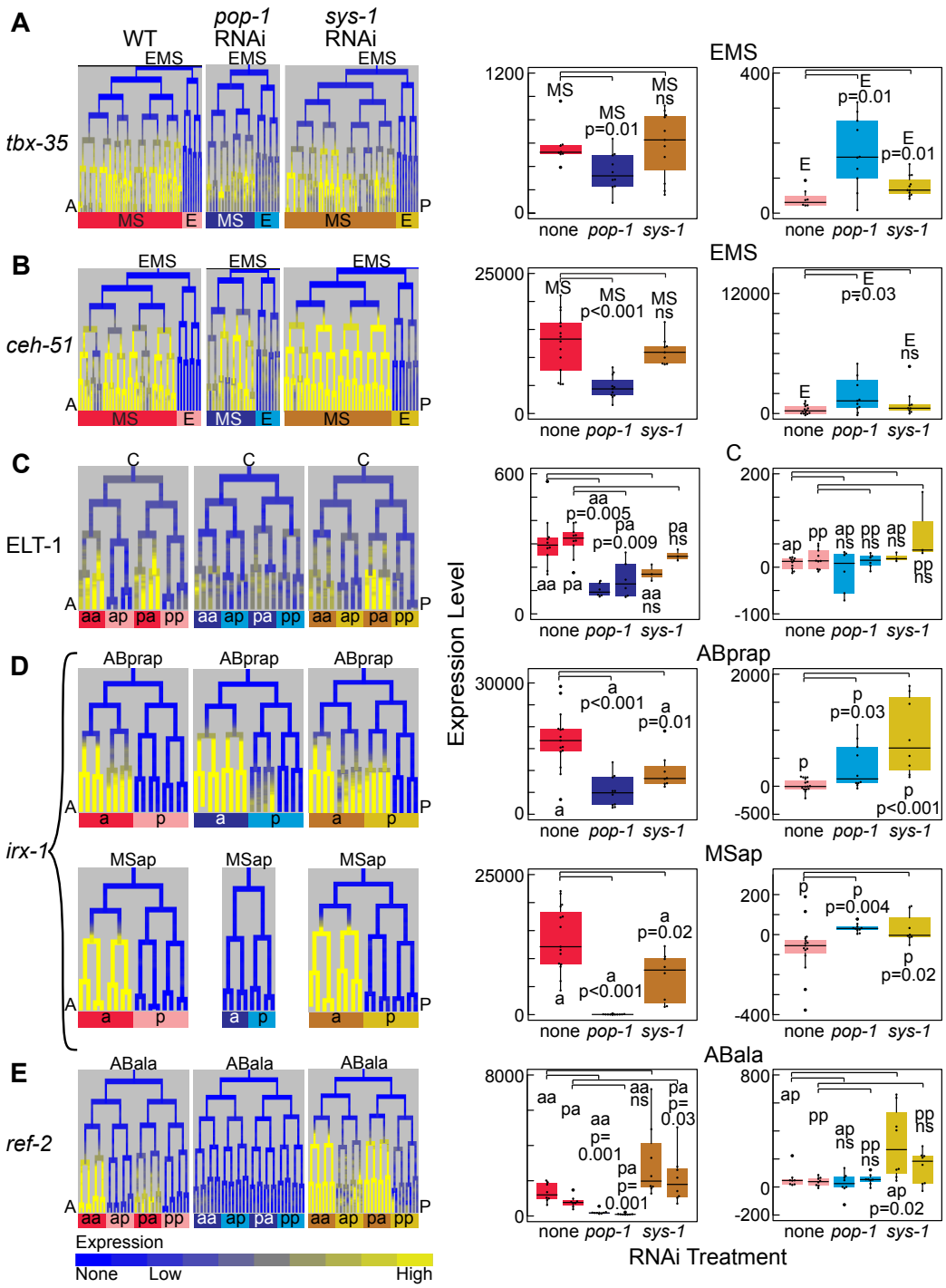

217

218 **Fig 3. Regulation of anterior genes by Wnt effectors *pop-1* and *sys-1*.**
219 (A-E) Expression pattern (left) and quantification (right) of reporters for the anterior genes *tbx-35*
220 (A), *ceh-51* (B), ELT-1 (C), *irx-1* (D), and *ref-2* (E) in specific anterior lineages and their posterior
221 sisters. Expression is shown under WT conditions and following *pop-1* or *sys-1* RNAi. Expression
222 quantification (right) is the mean expression across all measurements within that lineage from
223 when the reporter is normally first detected until the last time point indicated in the lineage (details
224 in Methods).

225 *irx-1* reporters are expressed early in four related anterior sublineages of ABp, and in three anterior
226 sublineages of MS, while in later embryos they are expressed in both anterior and posterior
227 lineages (Fig S3; Fig S4D). Like for *elt-1, pop-1* RNAi reduces *irx-1* reporter expression in anterior
228 ABp-derived sublineages, and two of the MS-derived expressing sublineages lose expression
229 nearly completely. After both *pop-1* and *sys-1* RNAi, the *irx-1* reporter expression expands into
230 several posterior sublineages of ABp whose anterior sisters normally express *irx-1* (Fig 3D; Fig
231 S4D; Table S4). These results indicate that *irx-1* requires *pop-1* for expression in anterior lineages
232 and both *pop-1* and *sys-1* for repression in posterior lineages.
233
234 Reporters for *ref-2* are expressed in the early embryo in all MS descendants and in several related
235 anterior sublineages of ABa that arise at the 50-cell stage (Fig S1; Fig S4E). In later embryos,
236 expression occurs in two anterior sublineages of MS, in several anterior ABp-derived sublineages,
237 and in the Pn ventral epidermal blast cells, consistent with previous studies [38]. After *pop-1*
238 RNAi, expression of the *ref-2* promoter reporter is significantly reduced in anterior sublineages of
239 ABala (Fig 3E). As for other genes, *sys-1* RNAi caused de-repression of *ref-2* in several posterior
240 sisters of the normally expressing sublineages, but we did not detect de-repression in these
241 sublineages after *pop-1* RNAi (Fig 3E; Fig S4E; Table S4). Thus, *ref-2* requires *pop-1* for
242 expression in anterior lineages and *sys-1* for repression in posterior lineages.
243
244 To summarize these perturbations, each anterior gene tested requires *pop-1* for full expression in
245 anterior lineages. Several genes also require *pop-1* (*tbx-35*, *ceh-51* and *irx-1*) or *sys-1* (*tbx-35, irx-*
246 *1* and *ref-2*) for repression in some posterior lineages. Thus, it appears that the expression of most
247 anterior genes requires the Wnt pathway components POP-1 and SYS-1, but this dependency is
248 complex as was seen previously for posterior genes [13].
249
250 **The anterior-specific transcription factor *ref-2/ZIC* is required for normal patterns of cell**
251 **division and cell position in expressing lineages.**
252
253 The striking anterior-specific expression patterns observed for early embryonic TFs raises the
254 question of whether these factors regulate the development of anterior lineages. To address this
255 question, we focused on one anterior gene, *ref-2*. *ref-2* encodes a zinc finger transcription factor

256 homologous to mammalian ZIC genes and *Drosophila* Odd-Paired. Previous work showed that
257 *ref-2* is required to prevent "Pn" epidermal blast cells from fusing with the major hypodermal
258 syncytium in larval stages [38]. More recently, REF-2 was shown to activate the anterior-specific
259 expression of the neural regulator *ttx-3* by binding the *ttx-3 cis*-regulatory region and recruiting
260 POP-1 in a manner independent of POP-1 DNA binding activity in the AIY mother cell [20]. Since
261 *ref-2* is expressed in many other anterior lineages in early embryos, we investigated whether *ref-2*
262 mutants have developmental defects in those lineages.
263
264 We tested for embryonic lineage phenotypes at single-cell resolution by analyzing 3D time-lapse
265 movies of eight embryos homozygous for the deletion allele *ref-2(gk178)* and expressing a
266 ubiquitous histone-mCherry fusion for cell tracking. We used StarryNite to track the lineage of
267 each embryo, and used AceTree to curate the lineages through the >550-cell stage (six embryos)
268 or >350-cell stage (two embryos). We compared the position and cell cycle length of each cell in
269 each embryo to those from a reference of 17 wild-type embryos [39,40] to identify outliers
270 ("defects") (Fig 4A).
271
272

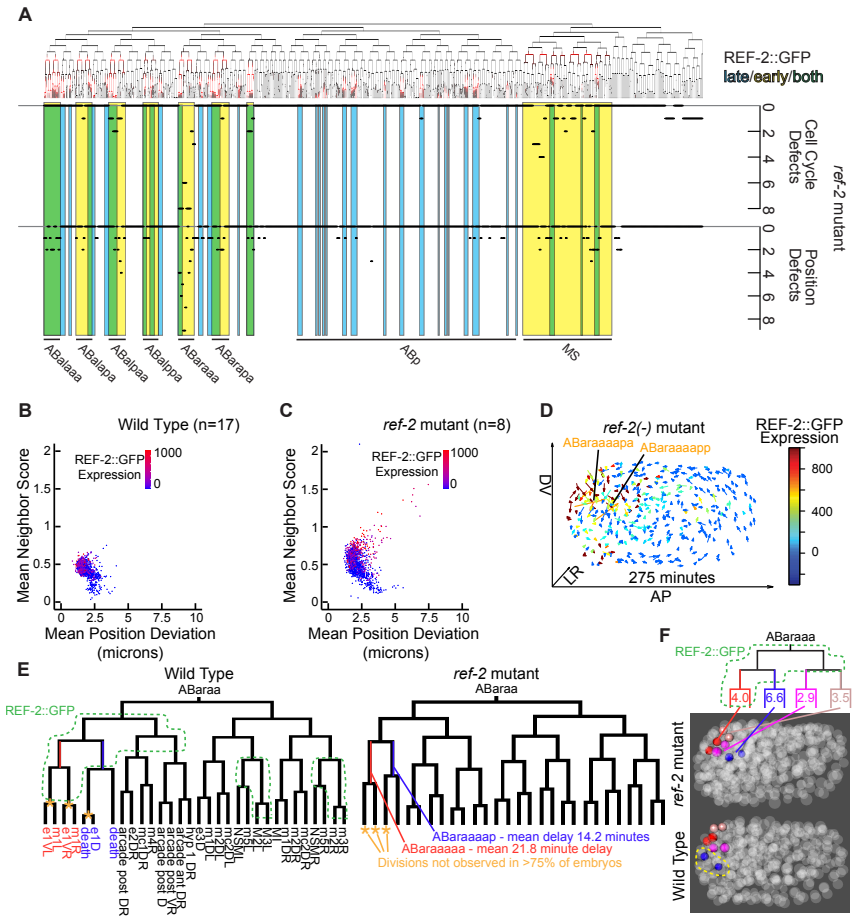

Fig 4. *ref-2* is required for proper division timing and positioning for many embryonic cells that are descended from cells that express *ref-2*.

(A) Lineage tree depicting the REF-2 protein expression pattern (top), and chart indicating the number of embryos out of eight homozygous *ref-2* mutant embryos that exhibit cell cycle defects and position defects in indicated cell lineages. Yellow indicates lineages that express *ref-2* early, blue indicates lineages that express *ref-2* late, and the overlap (green) indicates both. A corresponding analysis of wild-type embryos gives 0-1 defects per cell in all of 17 embryos tested [39]. (B-C) Scatter plot of mean neighbor score vs mean position deviation of cells of 17 wild-type (B) and eight *ref-2* mutant (C) embryos. Neighbor score is the ratio of each cell's distances to its ten closest wild-type neighbors between mutant and wild-type embryos. Points representing cells are colored based on WT REF-2::GFP expression levels [39]. (D) Plot of cell position deviations with arrows starting at the average WT position of cells and pointing to the average position in *ref-2* mutants. Arrows are colored by the WT expression levels of REF-2::GFP for each cell. The labeled cells (ABaraaaapa and ABaraaaapp) have the greatest mean cell position deviations. (E) ABaraa lineages of WT and *ref-2* mutant embryos, with cells expressing REF-2::GFP outlined on the WT tree. Two delayed and three missed cell divisions are highlighted on the *ref-2* mutant tree. (F) ABaraaa lineage with cells expressing REF-2::GFP outlined. The average position deviations in microns of terminal sister cells are indicated on the terminal branches of the lineage tree. Three dimensional projections of a WT and a *ref-2* mutant embryo are shown with the positions of the terminal ABaraaa lineage cells highlighted. ABaraaaapa and ABaraaaapp are outlined in the WT embryo projection as the cells with the greatest mean position deviation in the *ref-2* mutant.

296 We identified a total of 55 cells with early, late or missing divisions, and 54 of these were derived
297 from REF-2::GFP expressing lineages ($P < 10^{-15}$). Overall 95% of cell cycle defects were delays
298 or missed divisions, indicating a role for *ref-2* in promoting cell division. Similarly, we identified
299 68 position defects, of which 56 were in *ref-2* expressing lineages (Fig 4B, C, $P = 1.1 * 10^{-14}$, chi-
300 squared test). Ten *ref-2*-expressing cells, and no non-expressing cells, had position defects in two
301 or more embryos. The cells with the strongest position and cell cycle length defects were from the
302 *ref-2*-expressing anterior ABaraaa lineage, which produces primarily anterior pharynx cells (e1,
303 m1 and arcade cells). The most frequent cell cycle length defects were in ABaraaaaa and
304 ABaraaaap (both defective in 8 of 8 embryos), which were delayed by 21.8 minutes and 14.2
305 minutes, respectively (Fig 4E). The largest position defects were in ABaraaaapa and ABaraaaapp,
306 which were mispositioned on average 6 microns posterior of their wild-type position (Fig 4D,F).
307 However, other defects were broadly distributed across *ref-2*-expressing lineages, in particular
308 MS- and ABa-derived anterior sublineages (Fig 4A). In summary, the anterior lineage-expressed
309 TF *ref-2* is required for the normal development of anterior lineages, although the low penetrance
310 of many defects suggests that *ref-2* may act with other partially redundant regulators, similar to
311 other early zygotic TFs [39,41–46].
312
313 **Modular enhancers control *ref-2* embryonic expression**
314
315 The anterior expression and phenotypes of *ref-2* raise the question of what sequences and
316 regulators control this expression. To identify genomic sequences responsible for *ref-2* anterior
317 expression, we first compared expression driven by the 31.9 kb genomic fosmid protein reporter
318 to the shorter 4.1kb upstream ("promoter") reporter (Fig 5A, B, C; Fig S6). In general, the patterns
319 were similar; both are expressed broadly in the MS lineage and in multiple anterior ABa-derived
320 sublineages. In the ABa lineage, the promoter reporter shows background expression in some
321 posterior sister sublineages suggesting the existence of repressive sequences outside of this
322 promoter region. Additionally, the promoter fusion reporter is detected persistently in both the MS
323 and AB lineages, whereas protein reporter expression is detected transiently, likely reflecting the
324 use of a stable histone-mCherry reporter for the promoter reporter. Importantly, both the REF-
325 2::GFP protein and *ref-2* promoter reporters drive expression in progenitors of most cells defective
326 in *ref-2* mutants.

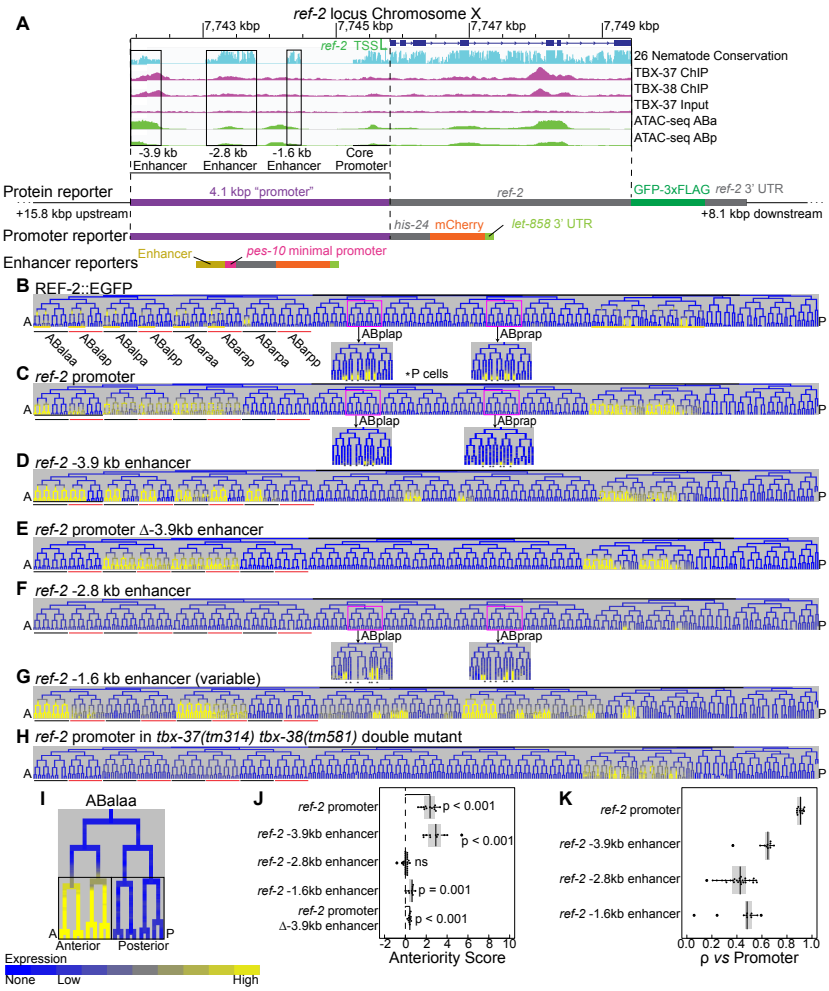

Fig 5. Identification of *ref-2* enhancers.

(A) Genome browser screenshot showing the *ref-2* locus on the X chromosome. Displayed tracks include the gene model, sequence conservation among 26 *Caenorhabditis* species [49], ChIP-seq data for TBX-37 and TBX-38 binding, and ATAC-seq data for cells in the ABa and ABp lineages [50]. Boxes indicate candidate enhancer regions as determined by conservation. Below the genome browser screenshot are models of the fluorescent reporter expression constructs we examined. (B-H) Lineage trees showing the expression patterns of *ref-2* protein (B), promoter (C), -3.9 kb enhancer reporter (D), promoter lacking the -3.9 kb enhancer (E), -2.8 kb enhancer reporter (F), -1.6 kb enhancer reporter (G), and promoter in the *tbx-37 tbx-38* double mutant (H) as determined by time-lapse confocal microscopy. Sublineages used in anteriority analyses are labeled in B and underlined in black (anterior) and red (posterior) under each lineage tree. Sublineages with transient early REF-2::EGFP (protein reporter) expression are underlined in yellow under the lineage tree in B. Pn ventral epidermal cells are indicated with asterisks in insets of panels B, C, and F. (I) Example lineage showing which cells were included in anteriority score analyses. Reporter expression levels were averaged across cells in the anterior or posterior lineages for the indicated cell generations. (J) Anteriority scores of the *ref-2* promoter, enhancers, and promoter lacking the -3.9 kb enhancer. Lineages used for analysis are ABala, ABalaa, ABalap, ABalpa, ABalpp, ABaraa, ABarap, ABarpa, and ABarpp (see Fig 5B). (K) Full somatic lineage correlation (Spearman's ρ) of each reporter's expression pattern with the mean expression pattern across embryos expressing the promoter reporter.

348 To identify the sequences in this region that regulate expression in these lineages, we sought to
349 identify minimal portions of the region with enhancer activity. We identified three portions of the
350 *ref-2* promoter conserved among *Caenorhabditis* species, suggesting they encode important
351 functions (Fig 5A) [47–49]. The most distal of these regions is in open chromatin in ABa-derived
352 cells as measured in a recently published ATAC-seq data set [50]. Also, this region is bound by
353 the broadly-expressed ABa lineage transcription factors TBX-37 and TBX-38, as determined by a
354 recently published ChIP-seq data set (Fig 5A) [50]. We fused each putative enhancer to a reporter
355 cassette consisting of a minimal *pes-10* promoter and a *his-24*::mCherry reporter. The *pes-10*
356 promoter is widely used, drives no consistent embryonic expression on its own [13,51,52] and is
357 compatible with a wide variety of enhancers [13,51]. We introduced each reporter into worms and
358 used StarryNite to determine in which cells each putative enhancer drives expression.
359
360 The most distal enhancer, located 3.9 kb upstream of the likely transcription start site, (-3.9 kb
361 enhancer; 449 base pairs) drives early expression (during gastrulation) in several anterior
362 sublineages of ABa and in anterior sublineages of MS (Fig 5D; Fig S6). This expression occurs in
363 nearly identical lineages to the early portion of the protein reporter expression pattern, but while
364 the protein reporter expression in these lineages is transient, the enhancer reporter persists, again
365 likely because of the use of a stable histone-mCherry reporter. The -3.9 kb enhancer expression is
366 also well correlated with the pattern driven by the full promoter of *ref-2* (Spearman's $\rho > 0.6$, Fig
367 5K). Deleting this enhancer from the *ref-2* promoter reporter results in loss of the strong anterior-
368 biased expression in the ABalaa, ABalap, and ABarpa lineages, and a loss in the weak anterior-
369 biased expression in the ABalpa, ABalpp, ABaraa, and ABarap lineages. All remaining consistent
370 expression occurs in the lineages derived from the Notch-signaled cells ABalp and ABara and has
371 little anterior bias (Fig 5E, J; Fig S5; Fig S6) [46]. The significance of this expression is unclear;
372 it can be seen in the promoter reporter but not the protein reporter, suggesting that it is normally
373 repressed by additional sequences outside the promoter. We conclude that the -3.9 kb enhancer is
374 necessary and sufficient for anterior-biased expression in the ABa lineage.
375
376 A second 745 bp enhancer, located at -2.8 kb, drives expression in later embryos (bean stage) in
377 some anterior sublineages of MS and in the ABp-derived Pn ventral epidermal blast cells that were
378 previously reported to require *ref-2* [38]. These cells also robustly express the *ref-2* protein reporter

379 and weakly express the *ref-2* promoter reporter (Fig 5B, C, F, J, K). Finally, the most proximal
380 enhancer candidate (at -1.6 kb; 206 base pairs) drives variable, weakly anterior-biased, expression
381 in multiple lineages, most consistently in ABala and ABara (Fig 5G, J, K; Fig S7) and also drives
382 late expression in some ABp sublineages (Fig 5G; Fig S7). Much of this expression is in cells or
383 at stages that do not express the full length reporters, suggesting that the activity of this sequence
384 differs in its normal genomic context.
385
386 To measure anterior expression bias we developed an "anteriority score" based on the log2 ratio
387 between anterior and posterior sister lineage expression. Because expression tends to accumulate
388 over several cell cycles in each expressing lineage, we calculated this score based on the mean
389 expression of the progeny 2-3 cell divisions after the birth of each anterior lineage (Fig 5I). Using
390 this metric, we detected robust and significant anterior-biased expression for both the *ref-2*
391 promoter and -3.9 kb enhancer reporters in ABa-derived sublineages, and reduced or no anterior-
392 biased expression for the -2.8 kb and -1.6 kb enhancer reporters and for the promoter Δ -3.9 kb
393 enhancer reporter in the same sublineages (Fig 5J). Comparing the expression driven by each
394 enhancer to the full promoter showed each is positively, but imperfectly, correlated, consistent
395 with each driving a subset of the full pattern (Fig 5K).
396
397 ***ref-2* promoter expression requires the T-box transcription factors *tbx-37* and *tbx-38***
398
399 A dominant feature of the early *ref-2* expression pattern is reiterated expression in six of the eight
400 anterior sister cells of the ectodermal ABa lineage at the 50 cell stage (when there are 16 ABa
401 descendants). This expression is not observed in the fluorescent reporter strains until at least the
402 following cell generation (when there are 32 ABa descendents) because of the time required for
403 the fluorophores of mCherry or GFP to mature. This raises the question of whether *ref-2* expression
404 requires the ABa-specific transcription factors *tbx-37* and *tbx-38*. These genes encode redundant
405 paralogous T-box family transcription factors which are expressed throughout the ABa lineage
406 and are required for multiple cell fate decisions within ABa [44,50,53]. Confirming previous
407 reports [44,50], a TBX-38::GFP knock-in reporter made by CRISPR [50] is expressed throughout
408 the ABa lineage and is detectable at least from the AB16 to AB128 stages (Fig S8). To test whether
409 *tbx-37* and *tbx-38* are necessary for *ref-2* expression, we measured expression of the *ref-2* promoter

410 reporter in embryos carrying homozygous deletions of both *tbx-37* and *tbx-38*. We found that in
411 the absence of *tbx-37* and *tbx-38,* nearly all *ref-2* promoter expression in the ABa lineage is lost
412 (Fig 5H; Fig S9), while expression in the MS lineage was maintained. Thus, *tbx-37* and *tbx-38* are
413 necessary for the anterior-biased expression of *ref-2* in ABa.
414
415 **The -3.9 kb enhancer contains three non-overlapping sub-enhancers that independently**
416 **drive anterior expression in the ABa lineage**
417
418 Since the *ref-2* -3.9 kb enhancer drives expression in a similar pattern to the early expression of
419 the full promoter and protein reporters, and its deletion from the *ref-2* promoter results in a
420 reduction of anterior-biased expression in portions of the ABa lineage, it is a primary enhancer
421 responsible for driving the early anterior-biased expression of *ref-2*. To map features necessary or
422 sufficient for anterior expression, we tested the activity of eight truncated versions of the *ref-2* -
423 3.9 kb enhancer to identify minimal regions of the enhancer sufficient to drive anterior expression
424 in the ABa lineage (Fig 6, Fig S10). Instead of a single minimal region, we found three non-
425 overlapping regions within the -3.9 kb enhancer that each are sufficient to drive anterior-biased
426 enhancer activity in the ABa lineage: a promoter-distal region (bases 1 to 200), a medial region
427 (bases 227 to 304) and a promoter-proximal region (bases 320 to 449) (Fig 6B, C). Of these
428 regions, the proximal region drives the most consistent expression and this expression is most
429 similar to the full length -3.9 kb enhancer construct (Fig 6D), whereas the medial and distal
430 fragments drive more variable expression and in a subset of these lineages. Thus, although
431 integration of information between these sub-enhancers is likely necessary for robustness of
432 expression pattern, the 130 bp proximal fragment provides a model system for further dissection
433 to identify anterior expression regulators.
434
435

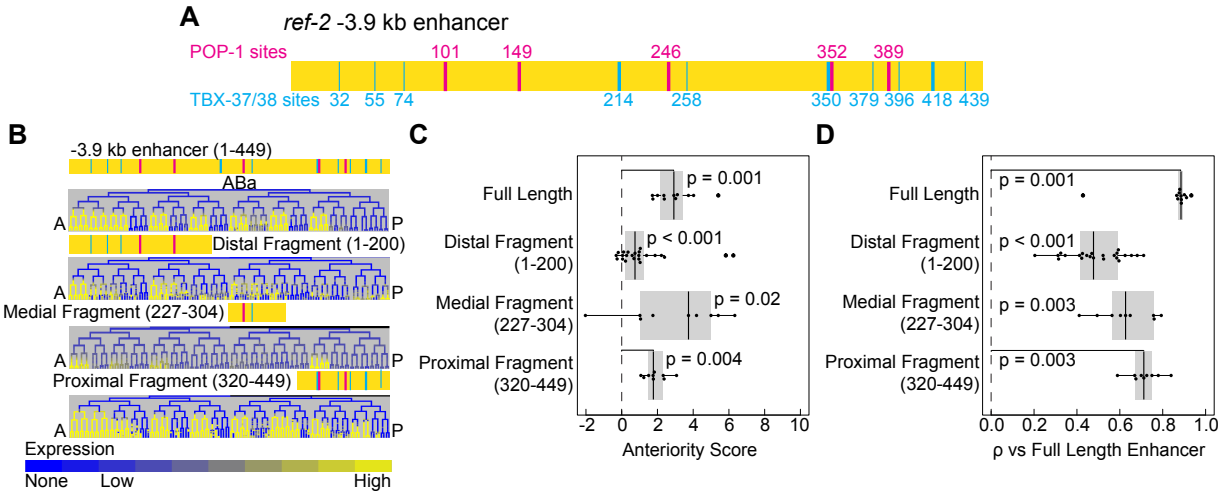

Fig 6. Three non-overlapping fragments of the -3.9 kb enhancer are each sufficient to drive anterior-biased expression in the ABa lineage of the early embryo.
(A) Model of the *ref-2* -3.9 kb enhancer with predicted TBX-37/38 sites (cyan, predicted high affinity sites indicated by thick line and predicted low-affinity by a thin line), and predicted high affinity POP-1 sites (magenta). (B) Expression patterns driven by full-length *ref-2* -3.9 kb enhancer and by minimal fragments. (C-D) Box plots displaying the anteriority scores (C) and Spearman's ρ (D) for the full-length *ref-2* -3.9 kb enhancer and minimal fragments. Lineages used to determine anteriority scores are the same as in Fig 5J. Spearman's ρ analysis uses the full ABa lineage and was calculated relative to the mean expression of the full-length -3.9 kb enhancer. A complete set of enhancer truncations tested is displayed in Fig S10.

TBX-37/38 binding sites are required for anterior expression of the proximal region

The proximal fragment exhibits broad sequence conservation with related nematodes, suggesting it contains multiple important TF binding sites (Fig 5A). To identify sequences necessary for anterior expression, we scrambled each 15 base-pair region along the length of the enhancer fragment and tested the resulting sequences for enhancer activity (Fig S11B, C, D). Scrambling a single region comprising base pairs 410-424 (coordinates relative to the full length enhancer) resulted in a complete loss of the anterior-biased expression in the ABa lineage, indicating that this region is necessary for this expression (Fig 7B; Fig S11B). Scrambling the most proximal regions 425-439 and 435-449 resulted in a loss of expression in subsets of the ABa lineage (in ABar and ABalp) but maintained anterior expression in the ABala lineage (Fig S11B). Expression was largely maintained when other regions were mutated, suggesting sequences in these regions are not individually necessary for anterior-specific expression despite their conservation.

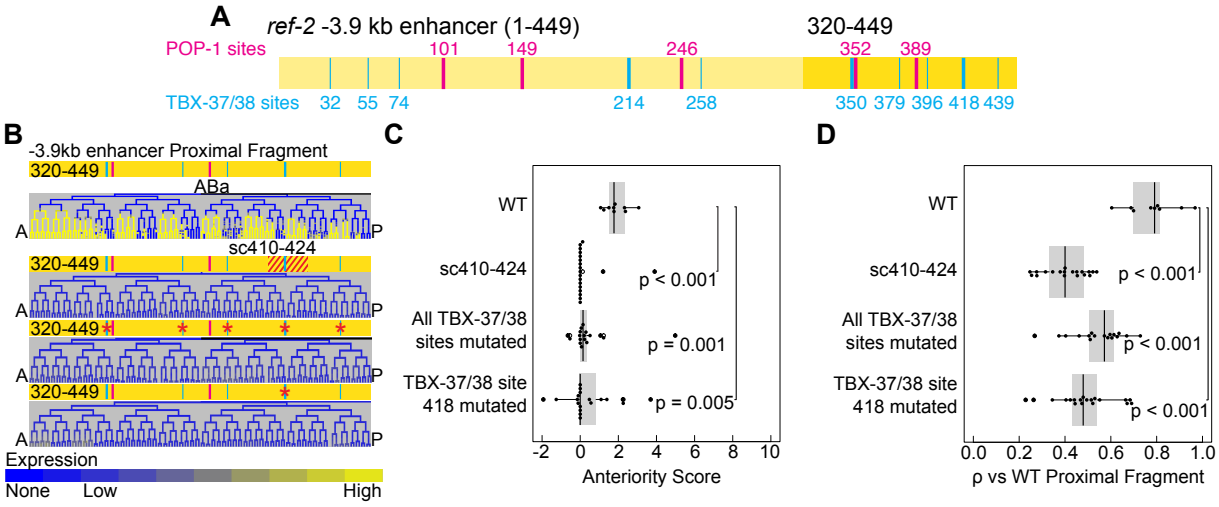

Fig 7. The ABa-expressed transcription factors *tbx-37* and *tbx-38* are required for the anterior-biased expression of *ref-2* in the ABa lineage.
(A) Model of the *ref-2* -3.9 kb enhancer with proximal fragment (base pairs 320-449) highlighted. Predicted TBX-37/38 and POP-1 sites are indicated as in Fig 6. (B) Expression patterns driven by the WT proximal fragment of the *ref-2* -3.9 kb enhancer, with base pairs 410-424 scrambled, with all predicted TBX-37/38 sites mutated, and TBX_{418} mutated. Expression driven by the proximal fragment with additional regions scrambled or with two predicted POP-1 sites mutated are displayed in Fig S11. (C-D) Anteriority scores (C) and Spearman's ρ (D) for the WT proximal fragment, with base pairs 410-424 scrambled, with all predicted TBX-37/38 sites mutated, and with TBX_{418} mutated. Lineages used to determine anteriority scores are the same as in Fig 5J. Spearman's ρ analysis uses the full ABa lineage and was calculated relative to the mean expression of the WT -3.9 kb enhancer proximal fragment.

In this fragment there are five predicted TBX-37/38 sites, two of which are predicted to have high affinity for TBX-37 and TBX-38. Two of the sites overlap with either the 410-424 region that is essential for ABa-specific expression or the 425-449 region that is required for a subset of ABa-specific expression (Fig 7A, B; Fig S11A, B). To determine whether this region is bound by TBX-37 and TBX-38 *in vivo,* we mined a recently published dataset that measured genome-wide TBX-37 and TBX-38 binding by ChIP-seq. Both factors show binding in the proximal region of the -3.9 kb enhancer (Fig 5A) [50].

To determine whether the TBX-37/38 sites are required for anterior expression, we measured the activity of the proximal fragment after mutating the two central nucleotides of all TBX-37/38 sites. The mutated enhancer fragment did not drive anterior-specific expression in the ABa lineage (Fig

489 7B, C, D; Fig S11B, C, D; Fig S12), confirming the importance of these sites. Additionally, the
490 loss of anterior-biased expression following the mutation of these sites indicates that the two
491 predicted high affinity POP-1 sites in this fragment are not sufficient to drive anterior-biased
492 expression. Also, these sites are not necessary for the anterior-biased expression driven by this
493 enhancer fragment, as the loss of these sites does not result in a loss of the anterior-biased
494 expression (Fig S11B, C, D). In fact, concatemers of POP-1 sites are sufficient to drive posterior-
495 biased expression (Fig S11F) [13,51].
496
497 Since the high affinity site beginning at position 418 (TBX_{418}) overlaps the region (410-424)
498 required for expression, we hypothesized that this specific TBX-37/38 site may be required for
499 anterior expression in the ABa lineage. To test this we tested the activity of the proximal fragment
500 with only the central two nucleotides of TBX_{418} mutated (Fig 7B, Fig S11B, E). This mutation
501 resulted in a loss of robust anterior-biased expression driven by the proximal fragment. Therefore,
502 TBX-37 and TBX-38 bind to the *ref-2* -3.9 kb enhancer proximal fragment and TBX_{418} is necessary
503 for it to drive robust anterior-biased expression (Fig 5A; Fig 7B, C, D; Fig S11B, C, D; Fig S12),
504 suggesting that TBX-37 and TBX-38 directly regulate *ref-2* expression.
505
506 **Concatemerized TBX sites are sufficient to drive anterior-specific expression in the ABa**
507 **lineage**
508
509 Given that *tbx-37* and *tbx-38* are expressed in both anterior and posterior cells within the ABa
510 lineage, we hypothesized that site TBX_{418} would be sufficient to drive broad expression in ABa,
511 with other sequences in the enhancer required for anterior specificity. To test this, we tested the
512 activity of synthetic enhancers comprising concatemerized copies of TBX_{418} separated by either
513 short (6-7 bp) or long (11-15 bp) flanking sequences from its endogenous context (Fig 8A).
514 Surprisingly, both of these reporters drove anterior-specific expression in the ABa lineage similar
515 to that driven by the full proximal fragment (Fig 8B, C, D). This indicates that either TBX_{418} or its
516 flanking sequences are sufficient both for ABa lineage expression, and for anterior-specific
517 expression within this lineage. To test the possibility that the flanking sequences are responsible
518 for anterior-specificity, we scrambled those sequences while leaving the central TBX_{418} site intact
519 in the context of the long-flanking-sequence construct. The resulting reporter was again expressed

only in anterior sublineages similar to the full proximal fragment (Fig 8A, B, C, D). Thus, when multimerized, TBX_{418} is sufficient both for ABa expression and for anterior specificity without additional non-overlapping sequences.

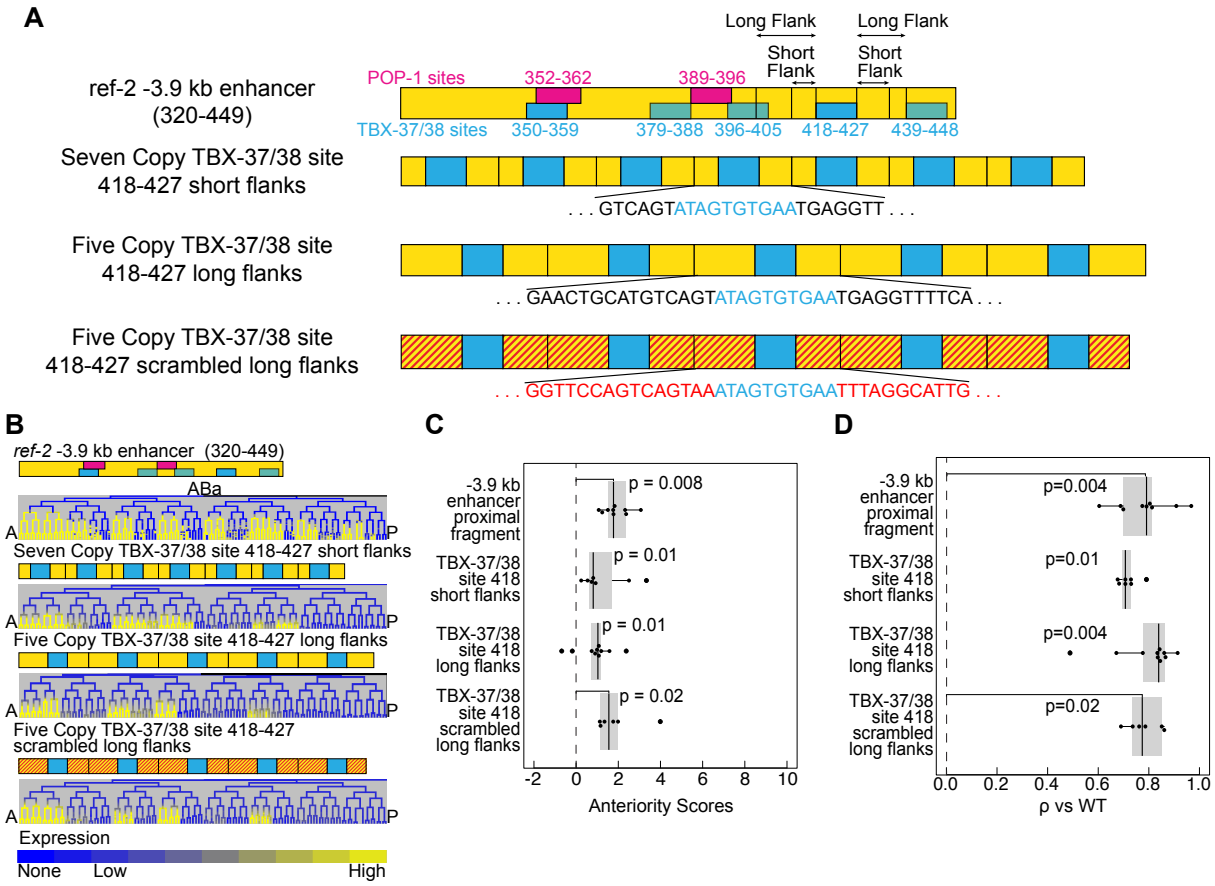

Fig 8. TBX_{418} in the *ref-2* -3.9 kb enhancer is sufficient when concatemerized to drive anterior-biased expression in the ABa lineage.
(A) Models of the proximal fragment of the *ref-2* -3.9 kb enhancer, the TBX_{418} seven-site concatemer with 6-7 base pair flanking regions, the TBX_{418} five-site concatemer with 11-15 base pair flanking regions, and the TBX_{418} five-site concatemer with 11-15 base pair scrambled flanking regions. (B) Expression patterns driven by the proximal fragment of the *ref-2* -3.9 kb enhancer and each TBX-37/38 site concatemer. (C-D) Anteriority scores (C) and Spearman's ρ (D) for the proximal fragment of the *ref-2* -3.9 kb enhancer and each TBX-37/38 binding site concatemer. Lineages used to determine anteriority scores are the same as in Fig 5J. Spearman's ρ analysis uses the full ABa lineage expression pattern and was calculated relative to the WT proximal fragment.

539 **DISCUSSION**

540

541 Previous work has definitively shown that the Wnt pathway components POP-1 and SYS-1
542 regulate posteriorly expressed genes in the *C. elegans* embryo via the canonical Wnt asymmetry
543 pathway [12,13,35]. What has been less clear is how the similar number of anteriorly expressed
544 genes are regulated. We have demonstrated that a set of anteriorly expressed genes, *tbx-35*, *ceh-*
545 *51*, *elt-1*, *irx-1*, and *ref-2*, require POP-1 and SYS-1 for their anterior-biased expression. Therefore,
546 POP-1 and SYS-1 regulate the expression of anterior-biased genes. The mechanism by which
547 POP-1 and SYS-1 mediate this regulation remains to be determined. Previous work demonstrated
548 that posterior genes can be regulated by POP-1 binding directly to POP-1 binding sites in their
549 upstream regulatory regions [51]. Thus, a simple indirect model of POP-1 regulation of anterior
550 genes would be POP-1 activating the expression of repressors in posterior cells. This mechanism
551 would predict that anterior genes would be expressed later than posterior genes, or that anterior
552 genes would be expressed early in both anterior and posterior cells, but maintained only in anterior
553 cells. This can happen; for example, in the C lineage *elt-1* is expressed in both anterior and
554 posterior sister cells at the 4C stage, but is only maintained in the anterior granddaughters of C
555 (Caa and Cpa), perhaps due to its repression by the Wnt target *hlh-1* in the descendents of the
556 posterior granddaughters of C (Cap and Cpp) [32]. What we observe in many cases, however, is
557 that anterior gene expression is activated at about the same time as posterior gene expression in
558 sister lineages. This observation suggests that POP-1 could regulate some anterior genes directly.
559 Although some *pop-1* dependence of anterior genes could be explained by upstream anterior-to-
560 posterior cell fate conversions following *pop-1* RNAi, our results as a whole cannot be explained
561 by the known pattern of fate transformations [44].

562

563 Indirect *pop-1*-dependent regulation of anterior genes, however, does not explain all of its role in
564 anterior gene expression regulation. For instance, previous work showed that loss of muscle-
565 specifying TFs (MRFs) expressed in Cap and Cpp (*hlh-1*, *unc-120*, and *hnd-1*) is not sufficient to
566 permit ectopic expression of *elt-1* in these cells or to convert them to an epidermal fate [32,54].
567 Therefore, another factor, perhaps *pop-1* acting directly, must be responsible for restricting *elt-1*
568 to the anterior C granddaughters. Our results identified a requirement for pop-1 in anterior
569 expression of elt-1 but not posterior repression in the C lineage. The proposed role of the MRFs in

570 repressing *elt-1* expression [32,54,55] suggests that this effect could partly be due to misexpression
571 of MRFs in the anterior C granddaughters, which could be tested in the future.
572
573 Direct activation of genes when Wnt is absent by POP-1/TCF, termed "opposite" Wnt target
574 regulation, occurs in other systems. For example, in *Drosophila* TCF bound directly to DNA at
575 non-optimal sites can activate transcription when unbound by β-catenin, and repress transcription
576 when bound to β-catenin. This difference in the regulatory activity of TCF is mediated by an
577 allosteric conformational change in the structure of TCF [22]. In *C. elegans*, POP-1 bound together
578 with REF-2 at the *ttx-3 cis*-regulatory region, may similarly undergo allosteric changes, leading to
579 opposite target regulation [20,21]. Our findings are consistent with a similar mechanism regulating
580 *ref-2* itself.
581
582 Our observation that five copies of a single 10 base-pair TBX-37/38 binding site are sufficient to
583 drive anterior-biased expression in the ABa lineage suggests that a POP-1 site is likely unnecessary
584 for anterior expression. However, *tbx-37* and *tbx-38* cannot explain this anterior bias alone, as
585 these factors are expressed throughout the ABa lineage. We showed that *pop-1* is required for both
586 anterior expression and posterior repression of the *ref-2* promoter. If this role of POP-1 is direct,
587 it likely acts by binding to other factors such as TBX-37 and TBX-38, rather than to DNA directly.
588 Consistent with this, TBX-38 and POP-1 were previously found to physically interact with each
589 other [56]. Intriguingly, several other T-box factors are expressed early in the AB lineage [50,57];
590 future work should determine if these play a role in restricting the activity of these sites to anterior
591 lineages. For instance, TBX_{418} is predicted to be bound by several other *C. elegans* T-box factors.
592 Other T-box factors expressed in the early ABa lineage could compete for binding at this site, with
593 POP-1 altering the relative activity of these factors between anterior and posterior cells.
594 Additionally, it is unclear whether *tbx-37* and *tbx-38* also regulate posterior gene expression in the
595 ABa lineage; intriguingly, the expression of *pha-4*, another anterior gene, in the ABa lineage is
596 also dependent on *tbx-37* and *tbx-38* [44].
597
598 In contrast with our observation that TBX_{418} concatemers are sufficient to drive anterior-biased
599 expression, Murgan et al. 2015 found that a REF-2 binding site concatemer is not sufficient to
600 drive expression in the anterior AIY mother cell. Instead, Murgan et al. identified binding sites for

601 helix-loop-helix family transcription factors that are sufficient to drive anterior expression in the
602 AIY mother and its posterior sister cell, and that combining these with REF-2 binding sites restricts
603 expression to the AIY mother. Thus, REF-2 acting through ZIC binding sites is not sufficient to
604 activate expression without cooperating factors binding other sites whereas TBX-37 and TBX-38
605 may be sufficient to do so. Other factors could also play a role, for example we used a pes-10
606 minimal promoter, whereas Murgan et al. did not include a minimal promoter in their constructs,
607 and there could be differences in sensitivity between the microscopy techniques.
608
609 Classic work in many species, including flies and vertebrates, has found that developmental genes
610 are often regulated both by partially redundant enhancers and modular enhancers that are
611 responsible for regulating distinct portions of the genes' expression patterns [58,59]. The extent to
612 which *C. elegans* genes are regulated by such distal enhancers vs promoter proximal elements has
613 been unclear. We found that the predicted enhancers in the promoter region of *ref-2* function
614 modularly, such that each enhancer drives different expression patterns, presumably providing
615 multiple inputs to fine-tune the expression pattern of *ref-2*. Combined with other recent studies
616 this adds to evidence that enhancer-mediated regulation is widespread during *C. elegans*
617 embryonic development [52,60–64]. Additionally, we observe modularity within the -3.9 kb
618 enhancer, with three non-overlapping regions of the enhancer each sufficient to drive anterior-
619 biased expression. Since the protein reporter is expressed in more lineages than the promoter
620 reporter, there are likely even more enhancers outside the promoter region that regulate expression
621 of *ref-2*.
622
623 Several studies have identified evidence for multiple functions of *ref-2*. *ref-2* was first identified
624 as being required for the production of the Pn.p ventral epidermal cells and for the inhibition of
625 their fusion to the epidermal syncytium hyp7 [38]. *ref-2* is also required for the initiation of the
626 differentiation of the cholinergic neuron AIY [65]. Also, *ref-2* has been found to be required for
627 female fate during sexual development [66]. We have demonstrated a role for *ref-2* in embryonic
628 development. *ref-2* is required for robust WT cell positioning and cell division timing in anterior
629 lineages. Intriguingly, an insect ortholog of *ref-2*, *odd-paired*, acts as a regulator of anterior-
630 posterior expression and is an anterior determinant in several species [67,68], suggesting the
631 function of *ref-2* in anterior fate regulation may be ancestral. Because the defects in cell position

632 and division timing are only partially penetrant, there are likely other, partially redundant
633 regulators of cell position and cell division timing that act with the sole *C. elegans* ZIC homolog
634 *ref-2* during embryonic development. Further experiments, including suppressor and enhancer
635 screens and co-mutation of other transcription factors will need to be performed to identify other
636 factors that regulate cell position and division timing in conjunction with *ref-2*.
637
638 **METHODS**
639
640 ***C. elegans* culture and strain generation**
641
642 *C. elegans* strains (Table S1) were maintained at standard growth temperatures on OP50 *E. coli*
643 on NGM plates (Table S2). RNAi knockdown was performed by feeding, as previously described
644 [69,70]. We validated the efficacy of *pop-1* RNAi by measuring the cell cycle delay resulting from
645 the transformation of the anterior MS lineage into an E-like lineage, and we validated the efficacy
646 of *sys-1* RNAi by failure of morphogenesis and embryonic death (Table S2) [13,33]. Enhancer
647 reporter strains were generated by microinjection into RW10029, the GFP histone strain used for
648 lineage tracing. Injection cocktails consisted of reporter DNA construct at 10 ng/μL, with 5 ng/μL
649 *myo-2*p::GFP, and 135 ng/μL pBluescript vector (or highest concentration possible whenever 135
650 ng/μL was impossible to make) and were injected using a Narishige MN-151 micromanipulator
651 with Tritech microinjector system. Other strains were created through crosses using standard
652 approaches (Table S1).
653
654 **Generation of transgenes**
655
656 Candidate enhancers were amplified by PCR from *C. elegans* N2 strain genomic DNA with
657 Phusion HF polymerase (New England Biosciences) and gel purified (Qiagen). Enhancer
658 fragments, mutated enhancers, and binding site concatemers were ordered as either gBlocks or
659 Ultramers from Integrated DNA Technologies (Coralville, Iowa) and were amplified with Phusion
660 HF polymerase (New England Biosciences) with overhangs for stitching and either gel or PCR
661 purified (Qiagen). Enhancer reporters were produced by fusing via PCR stitching these constructs
662 to a *pes-10* minimal promoter::HIS-24::mCherry::let-858 3'UTR fragment amplified from the

663 POPTOP plasmid [51] (Addgene #34848). The enhancer reporters were purified with a PureLink
664 PCR purification kit (ThermoFisher) and/or gel purified. The desired product was determined by
665 its size based on gel electrophoresis. We identified putative transcription factor binding sites using
666 CIS-BP (http://cisbp.ccbr.utoronto.ca) [71,72].To mutate the TBX-37/38 sites, the central two
667 nucleotides were altered (eg. ATAG**TG**TGAA changed to ATAG**GT**TGAA for *TBX*$_{418}$). For the
668 construct with all TBX-37/38 sites mutated, after mutating the five primary sites, subsequent
669 analysis revealed two weaker sites. All of these predicted TBX-37/38 sites were mutated. The
670 reporter construct for the *ref-2* promoter lacking the -3.9 kb enhancer was amplified from N2
671 genomic DNA by PCR and PCR stitched to the *pes-10* minimal promoter::HIS-24::mCherry
672 reporter, and, thus, drives expression through the *pes-10* minimal promoter. The *pes-10* promoter
673 drives no consistent embryonic expression on its own prior to elongation [13,51,52] and is
674 compatible with a wide variety of enhancers [13,51] (Table S5).
675
676 **Quantitative comparisons**
677
678 All quantitative comparisons were performed using R version 4.0.3 (The R Foundation for
679 Statistical Computing), Microsoft Excel version 16.16.27, or Python version 2.7.16. For the main
680 figures, a minimum N of 6 was used for all experiments, except for ELT-1::GFP expression after
681 *sys-1* RNAi, for which N = 3. For the supplemental figures, a minimum N of 2 was used (largely
682 for perturbations which appeared similar to wild-type at this level). Code and raw data for these
683 analyses are available at https://github.com/jisaacmurray/ref-2_paper.
684
685 *Expression and phenotypic analysis by 4D imaging*
686
687 We obtained confocal micrographs using a Leica TCS SP5 or Stellaris scanning confocal
688 microscope (67 z planes at 0.5 µm spacing and 1.5 minute time spacing, with laser power
689 increasing by 4-fold through the embryo depth to account for attenuation of signal with depth).
690 Embryos obtained from self-fertilized hermaphrodites were mounted in egg buffer/methyl
691 cellulose with 20µm beads used as spacers and imaged at 22°C using a stage temperature controller
692 (Brook Industries, Lake Villa, IL) [73]. We used StarryNite software to automatically annotate
693 nuclei and trace lineages [29]. We corrected errors from the automated analysis and quantified

694 reporter expression in each nucleus relative to the local background (using the "blot" background
695 correction technique) with AceTree software as previously described (Table S3) [24,26].
696
697 *Anterior gene WT to RNAi within lineage comparisons*
698
699 To compare the expression levels of the anterior genes *tbx-35*, *ceh-51*, ELT-1, *irx-1*, and *ref-2*
700 between WT and RNAi embryos within the expressing lineages and their posterior sisters, we
701 calculated for each embryo the mean reporter expression across all measurements within each
702 lineage (all descendant cells and time points) starting with the cell stage that expresses the reporter
703 at the time cells are born or shortly afterwards to the last time point in the indicated lineage. The
704 expression analyzed for the MS lineage starts at an earlier stage than that for other lineages, since
705 following *pop-1* RNAi the cell divisions are so dramatically delayed that reporter expression
706 comes on in earlier cell generations in these embryos. The cell generations used in each of these
707 comparisons are noted in Table S4.
708
709 *Anteriority Scores*
710
711 To measure the magnitude of anterior expression bias, we developed a measure that we refer to as
712 the anteriority score. To determine the anteriority scores, first we chose a minimum expression
713 cutoff and set all values below this cutoff to 0 and subtracted the minimum cutoff from all
714 expression values greater than or equal to the cutoff (an expression value of 200 was used as the
715 cutoff for all anteriority score analyses, except a value of zero was used for the TBX-38::GFP
716 reporter, which has very low fluorescence intensity compared to the other reporters analyzed).
717 Next, we averaged the expression levels of the reporter of interest in the cells of each anterior and
718 each posterior sister lineage of interest. For the *ref-2* promoter and enhancer constructs, as well as
719 the TBX-37/38 site concatemers, we analyzed anterior and posterior lineages descended from the
720 cells ABala, ABalaa, ABalap, ABalpa ABalpp ABaraa, ABarap, ABarpa, and ABarpp. We used
721 expression values starting at the generation with ABaxxxxxx cells (AB128 stage) until the time
722 point of the last division of AB128 stage cells in the ABa lineage. Next, we calculated the means
723 of the average expression levels of all of the anterior lineages and all of the posterior lineages
724 analyzed for each embryo. We then added a pseudocount of 1 to each of the anterior and posterior

725 embryo means. For each experimental group, the adjusted average anterior expression is divided
726 by the adjusted average posterior expression, and the base 2 logarithm of the result is reported--
727 Anteriority Score = $\log_2$((anterior mean + 1)/(posterior mean +1)).
728
729 *Correlation analysis*
730
731 Correlation analysis was done by Spearman's ρ, comparing each embryo's expression to the
732 average expression of the control group. Spearman's ρ was calculated in R using the "cor"
733 function. For Spearman's ρ we used all the data from the lineages of interest without excluding
734 any cell generations or having a minimum value cutoff. We included cells born before the onset
735 of expression here to include information about the cell generation of expression onset in the
736 analysis. For the analysis comparing the *ref-2* promoter with its enhancers we used the full somatic
737 lineage starting with the blastomeres AB, EMS, C, and D. For all other analyses we used only the
738 ABa lineage.
739
740 *Mutant cell position and cell division analysis*
741
742 We identified cell position and cell cycle defects as previously described [39]. We corrected for
743 differences in global division rates, and considered divisions as defective if they deviated from the
744 wild-type cell cycle length by at least five minutes and had a z-score greater than three. Cell
745 positions were corrected for differences in embryo size and rotation, and considered defective if
746 they deviated from the expected wild type position by at least five microns, had a z-score greater
747 than five, and a nearest neighbor score greater than 0.8.
748
749 *Statistical analyses*
750
751 Statistical significance of differences in anterior or posterior expression between untreated and
752 RNAi-treated embryos was tested using the two-tailed Wilcoxon Ranked Sum test. Statistical
753 significance of differences in Spearman's ρ or Anteriority Score were tested using the one-tailed
754 Wilcoxon Ranked Sum test to test for differences from either the control group or from 0, as
755 indicated in each figure. The p-values calculated by the Wilcoxon Ranked Sum test were corrected

756 for multiple comparisons using the false discovery rate method in R. Significance of overlap
757 between positional or cell division defects and expression status were assessed using a Chi-squared
758 test.
759
760

761 **FIGURES**

762

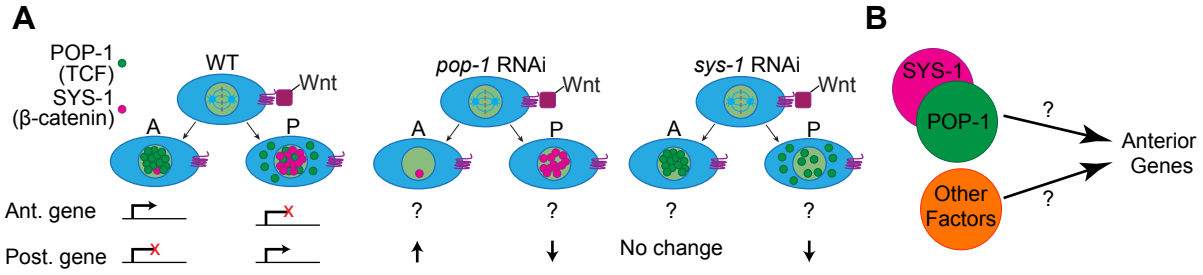

763
764

765 **Fig 1. How are anterior genes regulated?**

766 (A) The Wnt/β-catenin asymmetry pathway regulates anterior-posterior patterning by producing
767 asymmetric nuclear concentrations of POP-1/TCF and SYS-1/β-catenin in anterior and posterior
768 sister cells. Low nuclear concentrations of POP-1 and high nuclear concentrations of SYS-1 in the
769 posterior cell activate expression of posterior genes and are associated with the lack of expression
770 of anterior genes. Conversely, high nuclear concentrations of POP-1 and low nuclear
771 concentrations of SYS-1 in the anterior cell repress posterior genes and are associated with
772 expression of anterior genes. Effects of *pop-1* and *sys-1* RNAi on posterior genes are shown;
773 effects on most anterior genes are unknown. (B) In this work, we test whether *pop-1*/TCF and *sys-*
774 *1*/β-catenin regulate anterior genes in the *C. elegans* embryo, and ask what other factors also
775 regulate anterior expression.

776

777

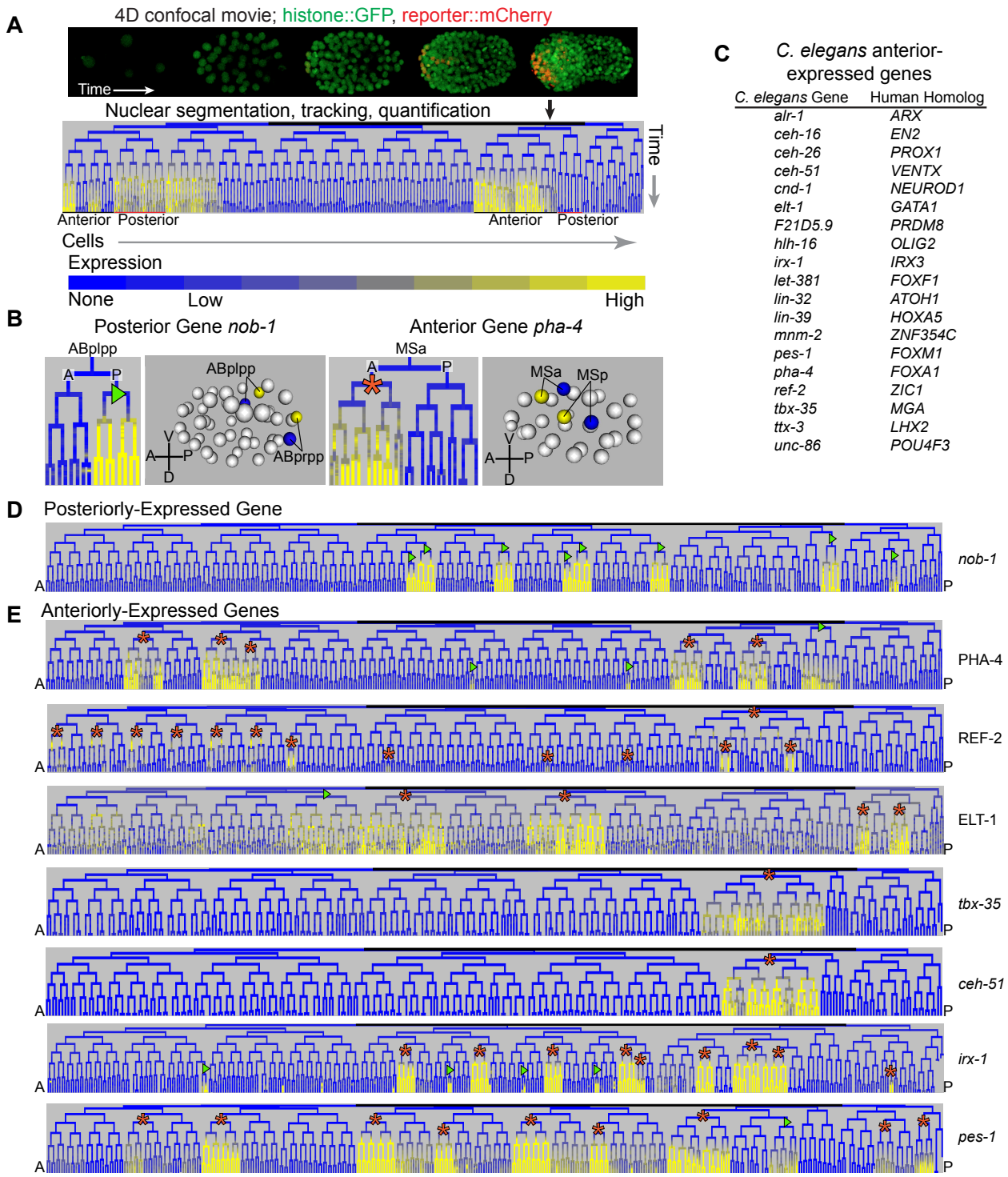

Fig 2. Identification of genes with anterior-biased expression.
(A) Automated lineaging traces lineages and quantifies expression from 4D confocal movies. In the lineage trees, vertical lines represent cells, and horizontal lines represent cell divisions. Most cells divide along the anterior-posterior axis, with anterior cells depicted on the left branch and posterior cells on the right branch. (B) Posterior and anterior genes are denoted as such based on their expression in cells descended from either a posterior or anterior sister cell, respectively,

786 following an anterior-posterior cell division. Anterior and posterior genes can generally be
787 expressed in cells from any part of the embryo. Anterior and posterior founder cells are labeled
788 with orange asterisks/green triangles respectively. (C) List of anterior-biased genes in the EPiC
789 database along with their predicted human homologs. (D) Expression pattern of a posterior gene,
790 *nob-1/Hox9-13*. (E) Expression patterns of several anterior genes; most are expressed in unique
791 combinations of mostly anterior lineages.
792
793

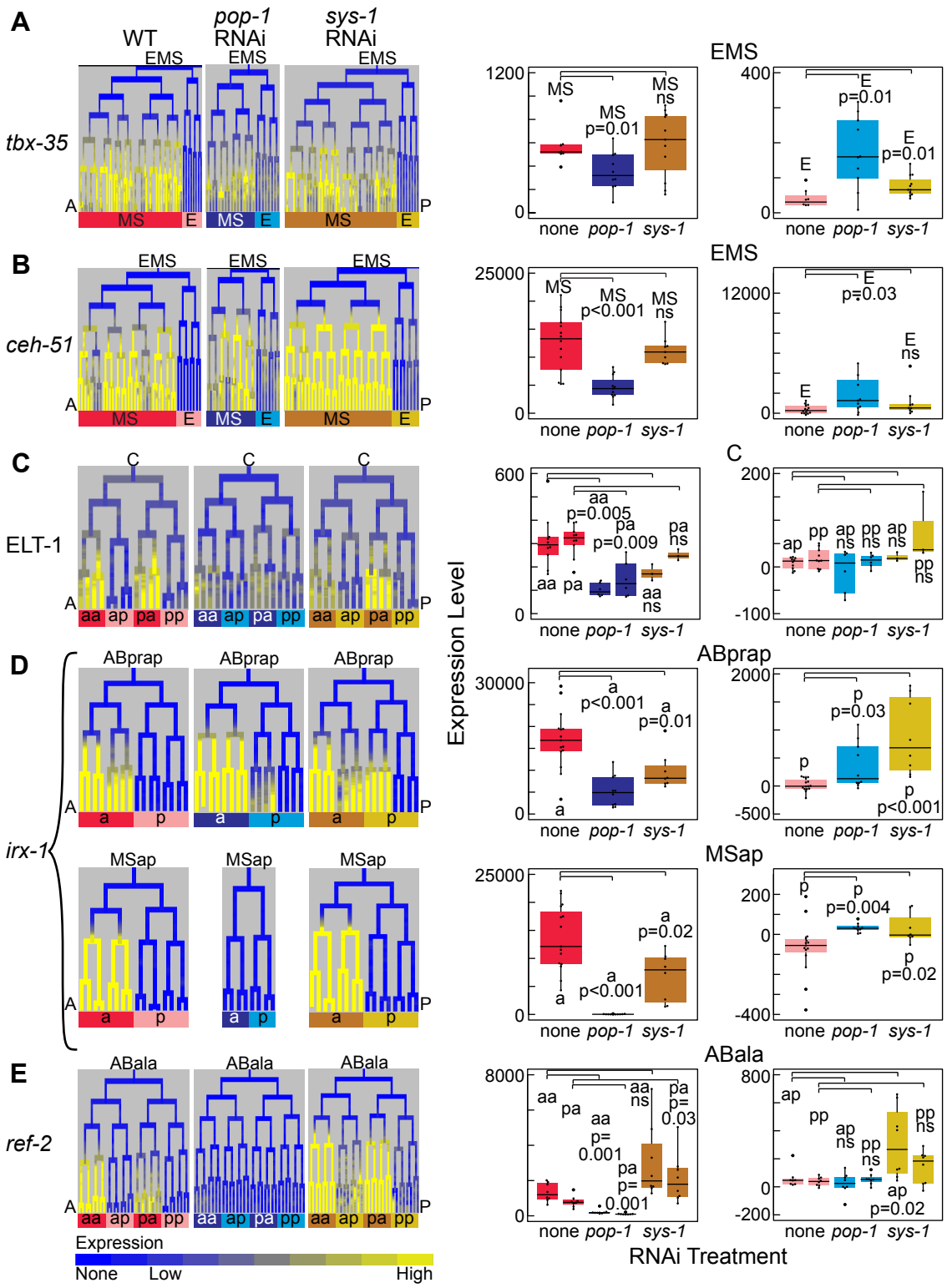

Fig 3. Regulation of anterior genes by Wnt effectors *pop-1* and *sys-1*.
(A-E) Expression pattern (left) and quantification (right) of reporters for the anterior genes *tbx-35* (A), *ceh-51* (B), ELT-1 (C), *irx-1* (D), and *ref-2* (E) in specific anterior lineages and their posterior sisters. Expression is shown under WT conditions and following *pop-1* or *sys-1* RNAi. Expression

quantification (right) is the mean expression across all measurements within that lineage from when the reporter is normally first detected until the last time point indicated in the lineage (details in Methods).

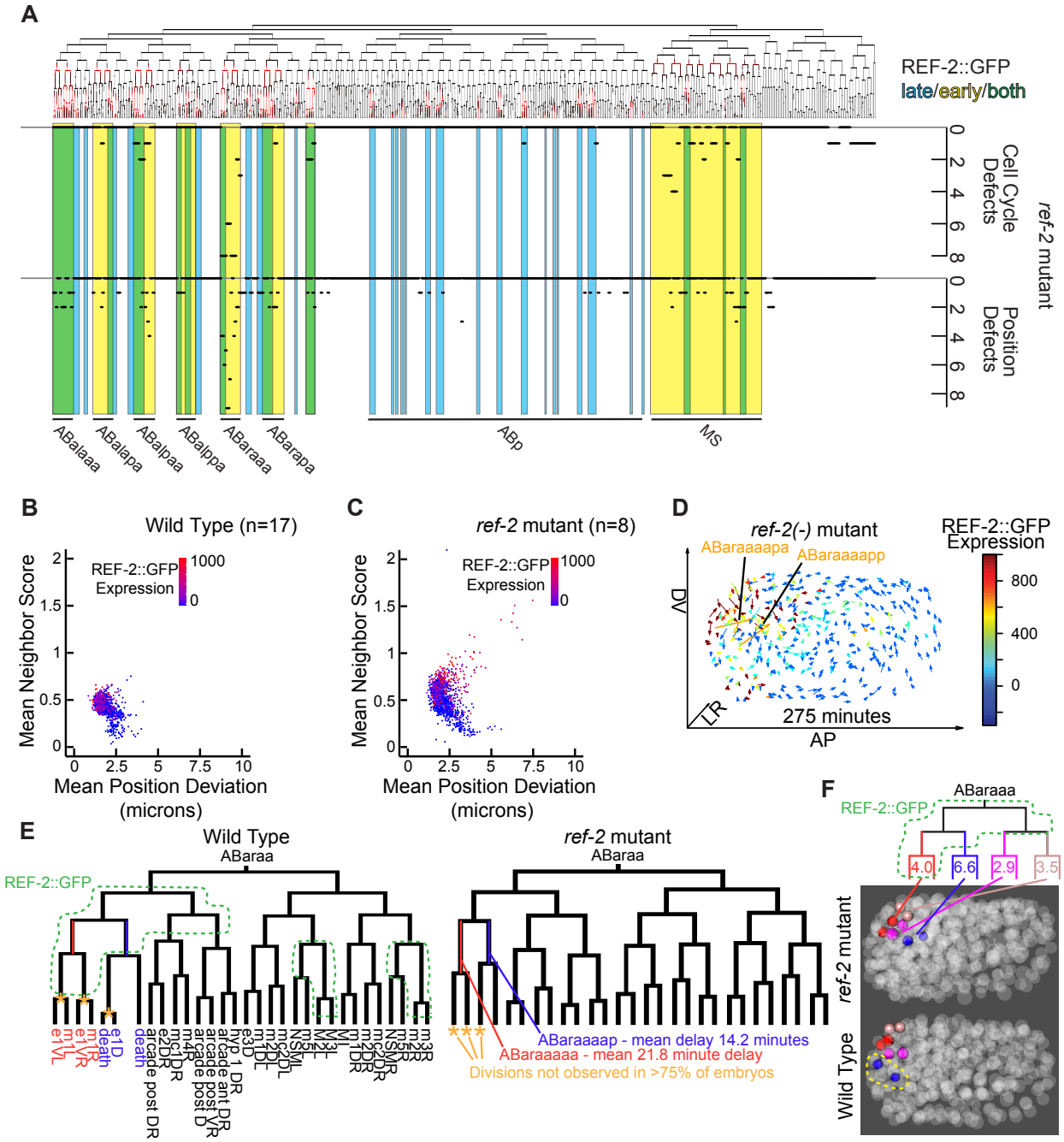

Fig 4. *ref-2* is required for proper division timing and positioning for many embryonic cells that are descended from cells that express *ref-2*.

(A) Lineage tree depicting the REF-2 protein expression pattern (top), and chart indicating the number of embryos out of eight homozygous *ref-2* mutant embryos that exhibit cell cycle defects and position defects in indicated cell lineages. Yellow indicates lineages that express *ref-2* early, blue indicates lineages that express *ref-2* late, and the overlap (green) indicates both. A corresponding analysis of wild-type embryos gives 0-1 defects per cell in all of 17 embryos tested [39]. (B-C) Scatter plot of mean neighbor score vs mean position deviation of cells of 17 wild-type (B) and eight *ref-2* mutant (C) embryos. Neighbor score is the ratio of each cell's distances to its

ten closest wild-type neighbors between mutant and wild-type embryos. Points representing cells are colored based on WT REF-2::GFP expression levels [39]. (D) Plot of cell position deviations with arrows starting at the average WT position of cells and pointing to the average position in *ref-2* mutants. Arrows are colored by the WT expression levels of REF-2::GFP for each cell. The labeled cells (ABaraaaapa and ABaraaaapp) have the greatest mean cell position deviations. (E) ABaraa lineages of WT and *ref-2* mutant embryos, with cells expressing REF-2::GFP outlined on the WT tree. Two delayed and three missed cell divisions are highlighted on the *ref-2* mutant tree. (F) ABaraaa lineage with cells expressing REF-2::GFP outlined. The average position deviations in microns of terminal sister cells are indicated on the terminal branches of the lineage tree. Three dimensional projections of a WT and a *ref-2* mutant embryo are shown with the positions of the terminal ABaraaa lineage cells highlighted. ABaraaaapa and ABaraaaapp are outlined in the WT embryo projection as the cells with the greatest mean position deviation in the *ref-2* mutant.

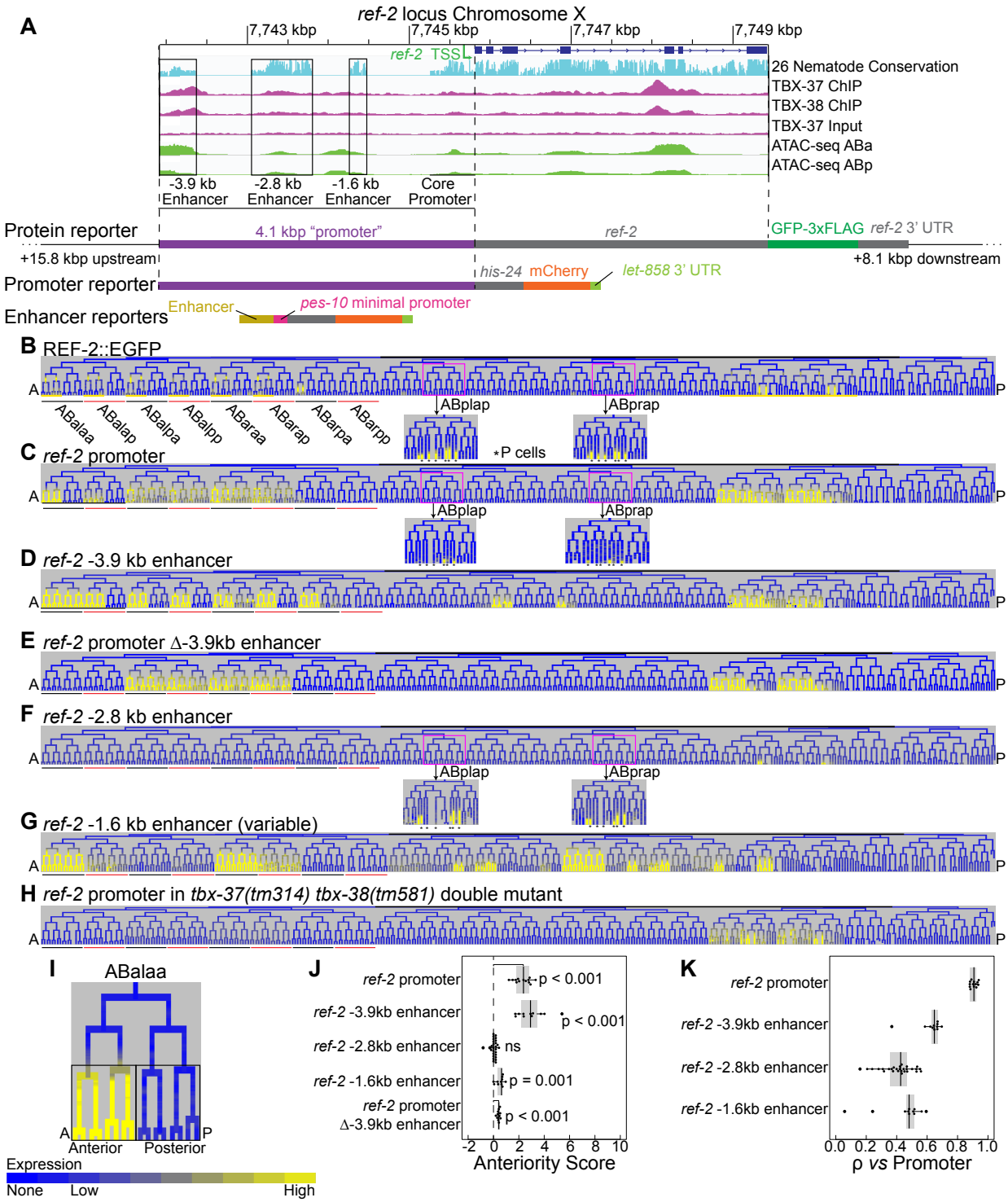

Fig 5. Identification of *ref-2* enhancers.

(A) Genome browser screenshot showing the *ref-2* locus on the X chromosome. Displayed tracks include the gene model, sequence conservation among 26 *Caenorhabditis* species [49], ChIP-seq data for TBX-37 and TBX-38 binding, and ATAC-seq data for cells in the ABa and ABp lineages [50]. Boxes indicate candidate enhancer regions as determined by conservation. Below the genome browser screenshot are models of the fluorescent reporter expression constructs we examined. (B-

838 H) Lineage trees showing the expression patterns of *ref-2* protein (B), promoter (C), -3.9 kb
839 enhancer reporter (D), promoter lacking the -3.9 kb enhancer (E), -2.8 kb enhancer reporter (F), -
840 1.6 kb enhancer reporter (G), and promoter in the *tbx-37 tbx-38* double mutant (H) as determined
841 by time-lapse confocal microscopy. Sublineages used in anteriority analyses are labeled in B and
842 underlined in black (anterior) and red (posterior) under each lineage tree. Sublineages with
843 transient early REF-2::EGFP (protein reporter) expression are underlined in yellow under the
844 lineage tree in B. Pn ventral epidermal cells are indicated with asterisks in insets of panels B, C,
845 and F. (I) Example lineage showing which cells were included in anteriority score analyses.
846 Reporter expression levels were averaged across cells in the anterior or posterior lineages for the
847 indicated cell generations. (J) Anteriority scores of the *ref-2* promoter, enhancers, and promoter
848 lacking the -3.9 kb enhancer. Lineages used for analysis are ABala, ABalaa, ABalap, ABalpa,
849 ABalpp, ABaraa, ABarap, ABarpa, and ABarpp (see Fig 5B). (K) Full somatic lineage correlation
850 (Spearman's ρ) of each reporter's expression pattern with the mean expression pattern across
851 embryos expressing the promoter reporter.
852
853

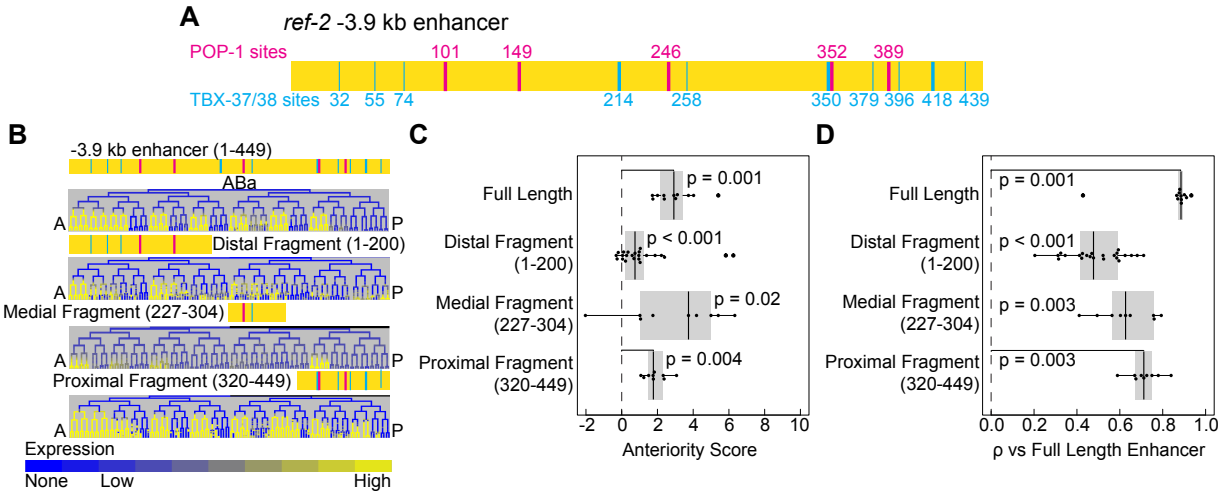

Fig 6. Three non-overlapping fragments of the -3.9 kb enhancer are each sufficient to drive anterior-biased expression in the ABa lineage of the early embryo.
(A) Model of the *ref-2* -3.9 kb enhancer with predicted TBX-37/38 sites (cyan, predicted high affinity sites indicated by thick line and predicted low-affinity by a thin line), and predicted high affinity POP-1 sites (magenta). (B) Expression patterns driven by full-length *ref-2* -3.9 kb enhancer and by minimal fragments. (C-D) Box plots displaying the anteriority scores (C) and Spearman's ρ (D) for the full-length *ref-2* -3.9 kb enhancer and minimal fragments. Lineages used to determine anteriority scores are the same as in Fig 5J. Spearman's ρ analysis uses the full ABa lineage and was calculated relative to the mean expression of the full-length -3.9 kb enhancer. A complete set of enhancer truncations tested is displayed in Fig S10.

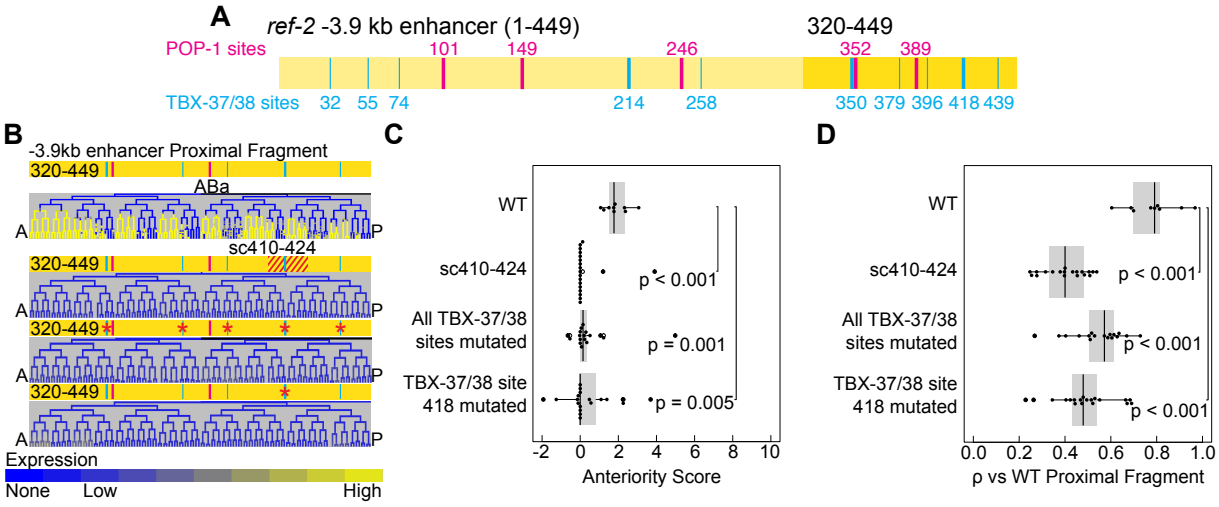

Fig 7. The ABa-expressed transcription factors *tbx-37* and *tbx-38* are required for the anterior-biased expression of *ref-2* in the ABa lineage.

(A) Model of the *ref-2* -3.9 kb enhancer with proximal fragment (base pairs 320-449) highlighted. Predicted TBX-37/38 and POP-1 sites are indicated as in Fig 6. (B) Expression patterns driven by the WT proximal fragment of the *ref-2* -3.9 kb enhancer, with base pairs 410-424 scrambled, with all predicted TBX-37/38 sites mutated, and TBX_{418} mutated. Expression driven by the proximal fragment with additional regions scrambled or with two predicted POP-1 sites mutated are displayed in Fig S11. (C-D) Anteriority scores (C) and Spearman's ρ (D) for the WT proximal fragment, with base pairs 410-424 scrambled, with all predicted TBX-37/38 sites mutated, and with TBX_{418} mutated. Lineages used to determine anteriority scores are the same as in Fig 5J. Spearman's ρ analysis uses the full ABa lineage and was calculated relative to the mean expression of the WT -3.9 kb enhancer proximal fragment.

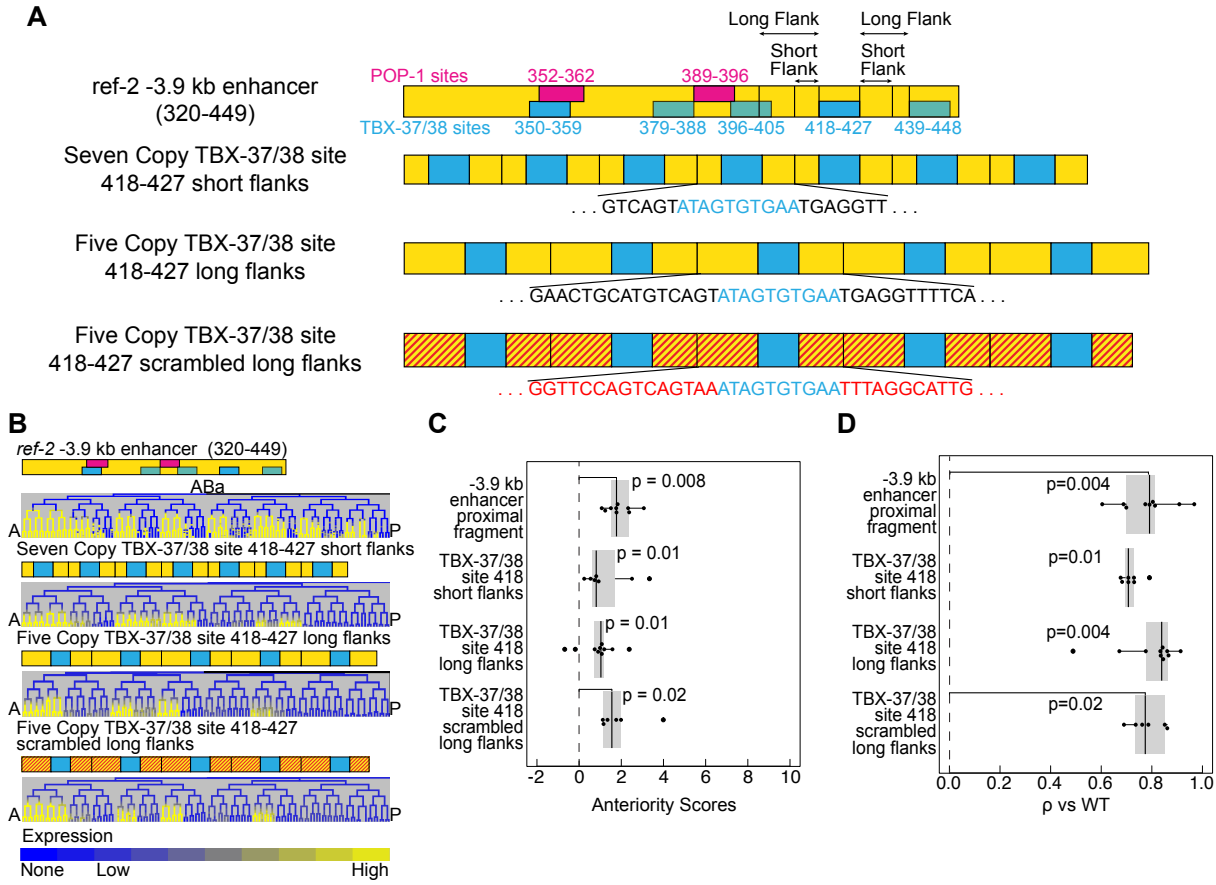

Fig 8. *TBX$_{418}$* in the *ref-2* -3.9 kb enhancer is sufficient when concatemerized to drive anterior-biased expression in the ABa lineage.
(A) Models of the proximal fragment of the *ref-2* -3.9 kb enhancer, the *TBX$_{418}$* seven-site concatemer with 6-7 base pair flanking regions, the *TBX$_{418}$* five-site concatemer with 11-15 base pair flanking regions, and the *TBX$_{418}$* five-site concatemer with 11-15 base pair scrambled flanking regions. (B) Expression patterns driven by the proximal fragment of the *ref-2* -3.9 kb enhancer and each TBX-37/38 site concatemer. (C-D) Anteriority scores (C) and Spearman's ρ (D) for the proximal fragment of the *ref-2* -3.9 kb enhancer and each TBX-37/38 binding site concatemer. Lineages used to determine anteriority scores are the same as in Fig 5J. Spearman's ρ analysis uses the full ABa lineage expression pattern and was calculated relative to the WT proximal fragment.

ref-2 REF-2 *elt-1* ELT-1

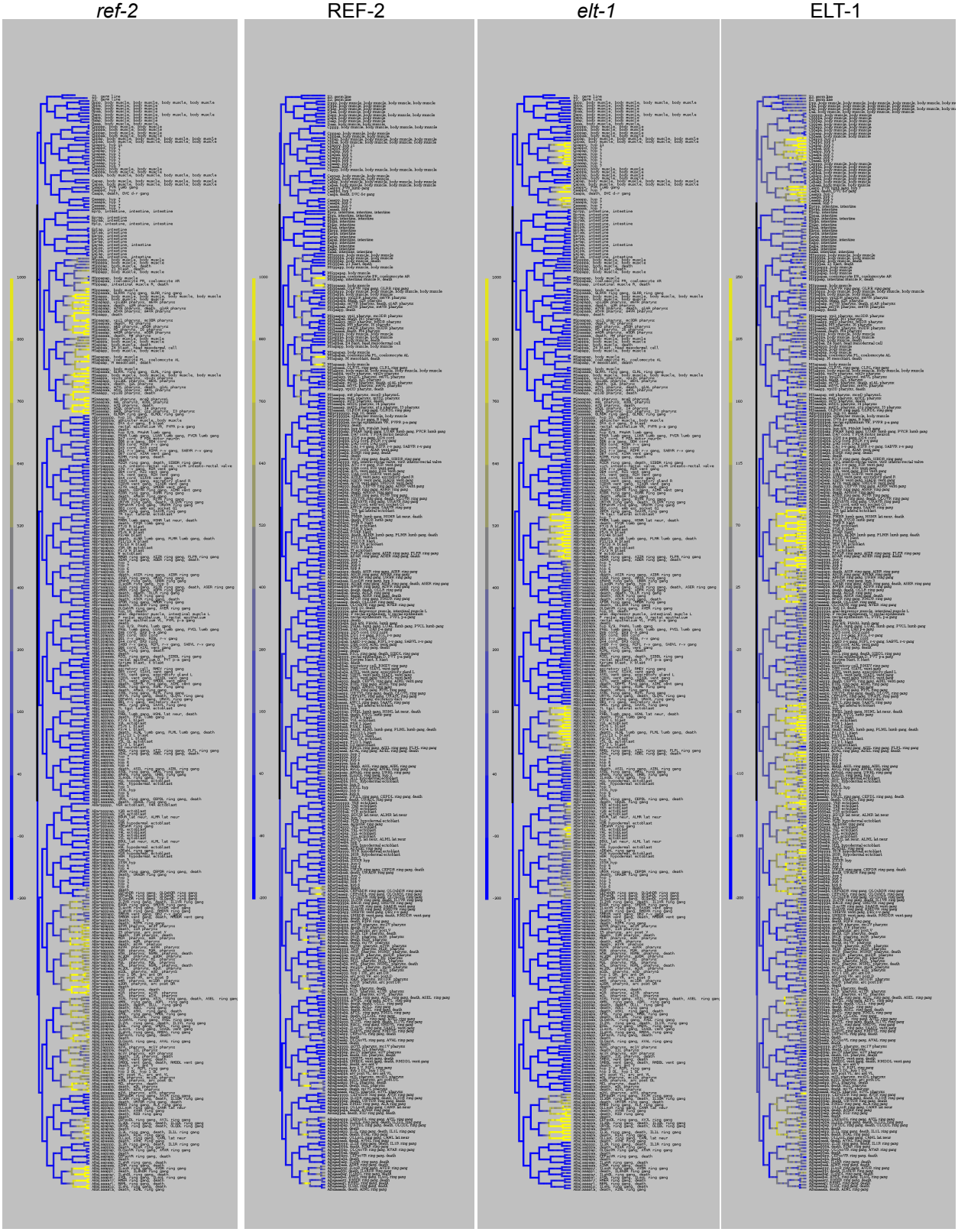

895
896
897

898 **Fig S1. Several early embryonic genes are expressed with anterior bias.**
899 Full lineage expression patterns are shown for integrated transgenic promoter reporters of *ref-2*
900 and *elt-1*; and for integrated transgenic protein reporters of REF-2 and ELT-1.

tbx-35 *ceh-51* CEH-51 PHA-4

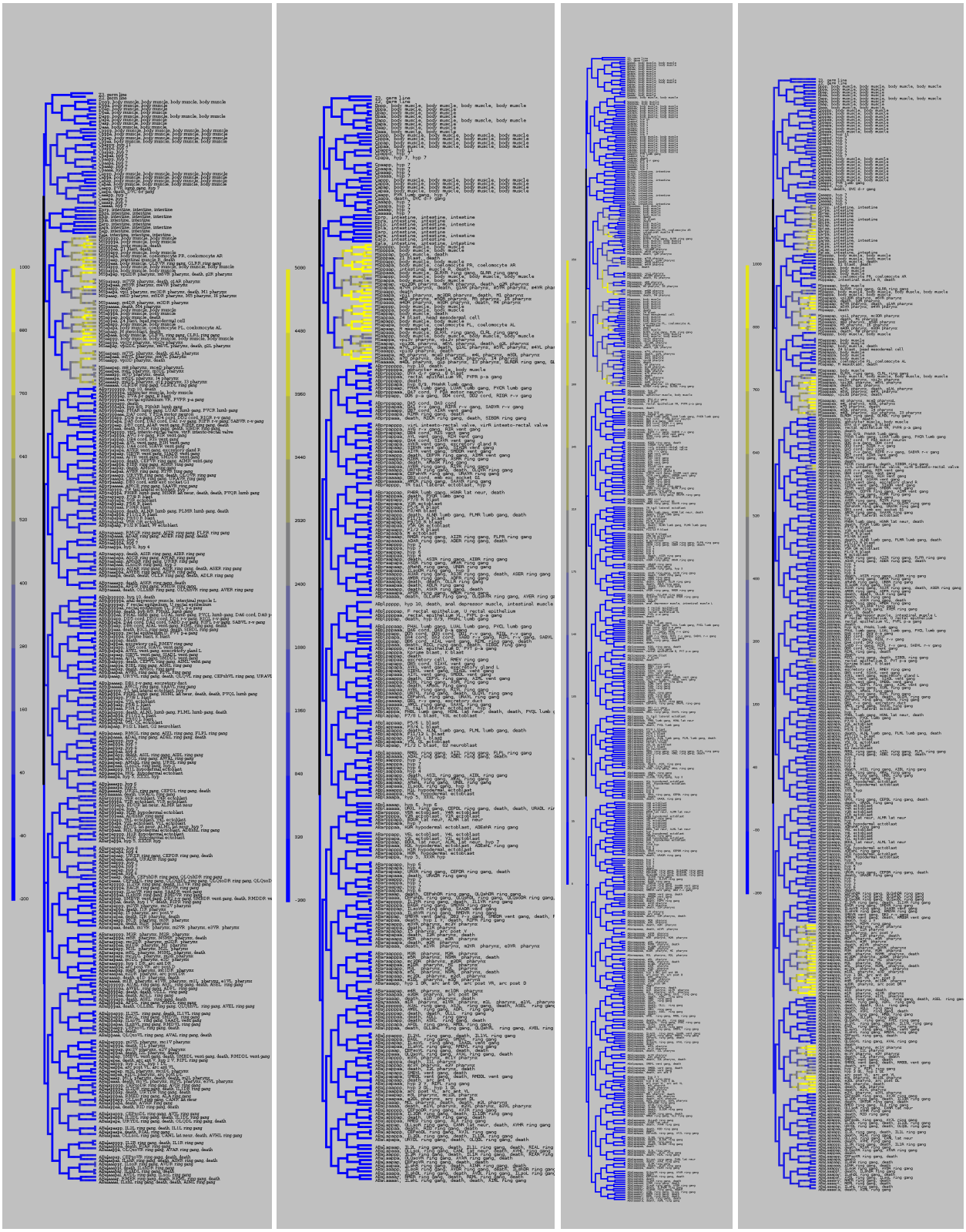

901
902
903

904 **Fig S2. Several early embryonic genes are expressed with anterior bias.**
905 Full lineage expression patterns are shown for integrated transgenic promoter reporters of *tbx-35*
906 and *ceh-51*; for an integrated transgenic protein reporter of PHA-4; and for a CRISPR knock-in
907 protein reporter of CEH-51.

irx-1 IRX-1 *pes-1*

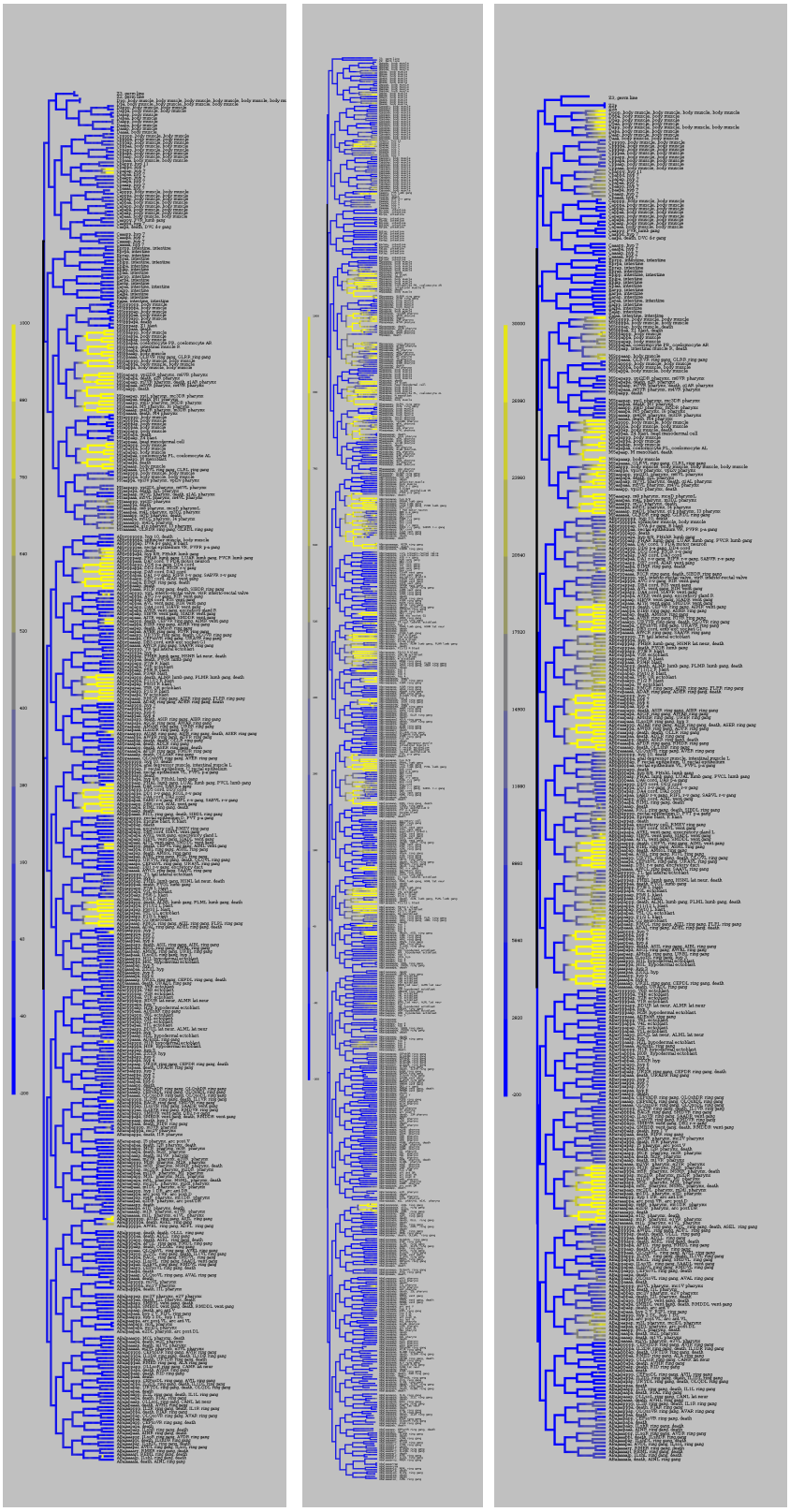

908
909
910

911 **Fig S3. Several early embryonic genes are expressed with anterior bias.**
912 Full lineage expression patterns are shown for integrated transgenic promoter reporters of *irx-1*
913 and *pes-1*; and for an integrated transgenic protein reporter of IRX-1.
914
915

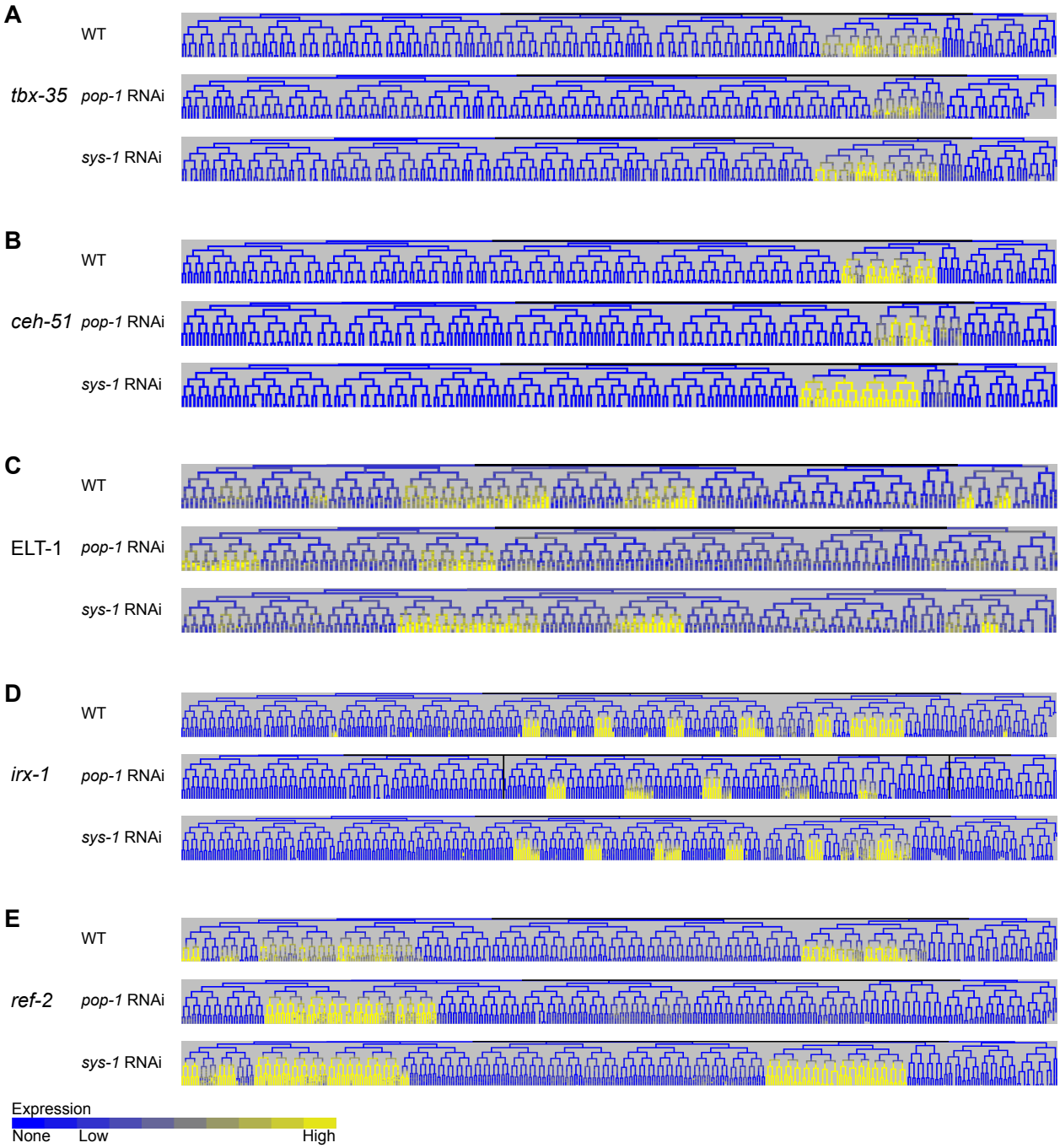

Fig S4. Anterior genes are regulated by Wnt effectors *pop-1* and *sys-1*.
Full example WT, *pop-1* RNAi, and *sys-1* RNAi lineages are shown for integrated transgenic promoter reporters of *tbx-35* (A), *ceh-51* (B), *irx-1* (D), and *ref-2* (E) and for an integrated transgenic protein reporter of ELT-1 (C).

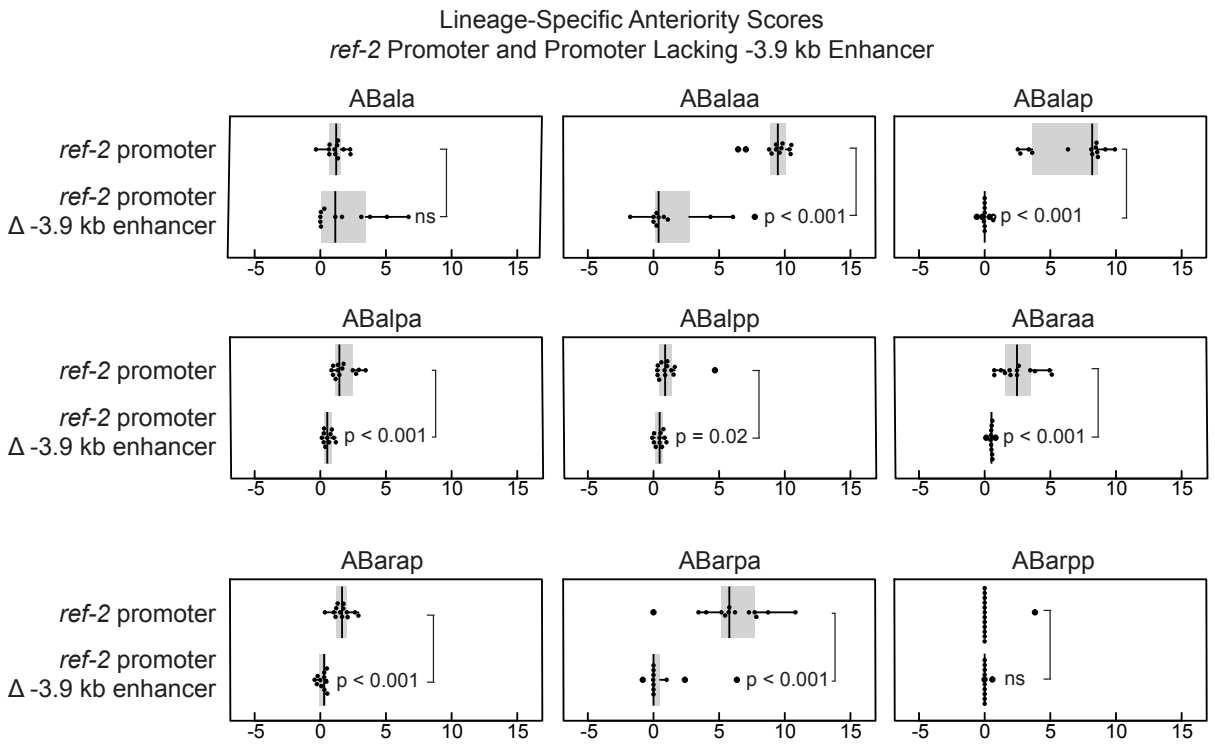

Fig S5. Deletion of the -3.9 kb enhancer from the *ref-2* promoter causes a reduction in the anterior bias in the expression driven by the promoter in most ABa sublineages in which the full-length promoter drives anterior-biased expression.

Box plots display anteriority scores of lineages descended from indicated cells.

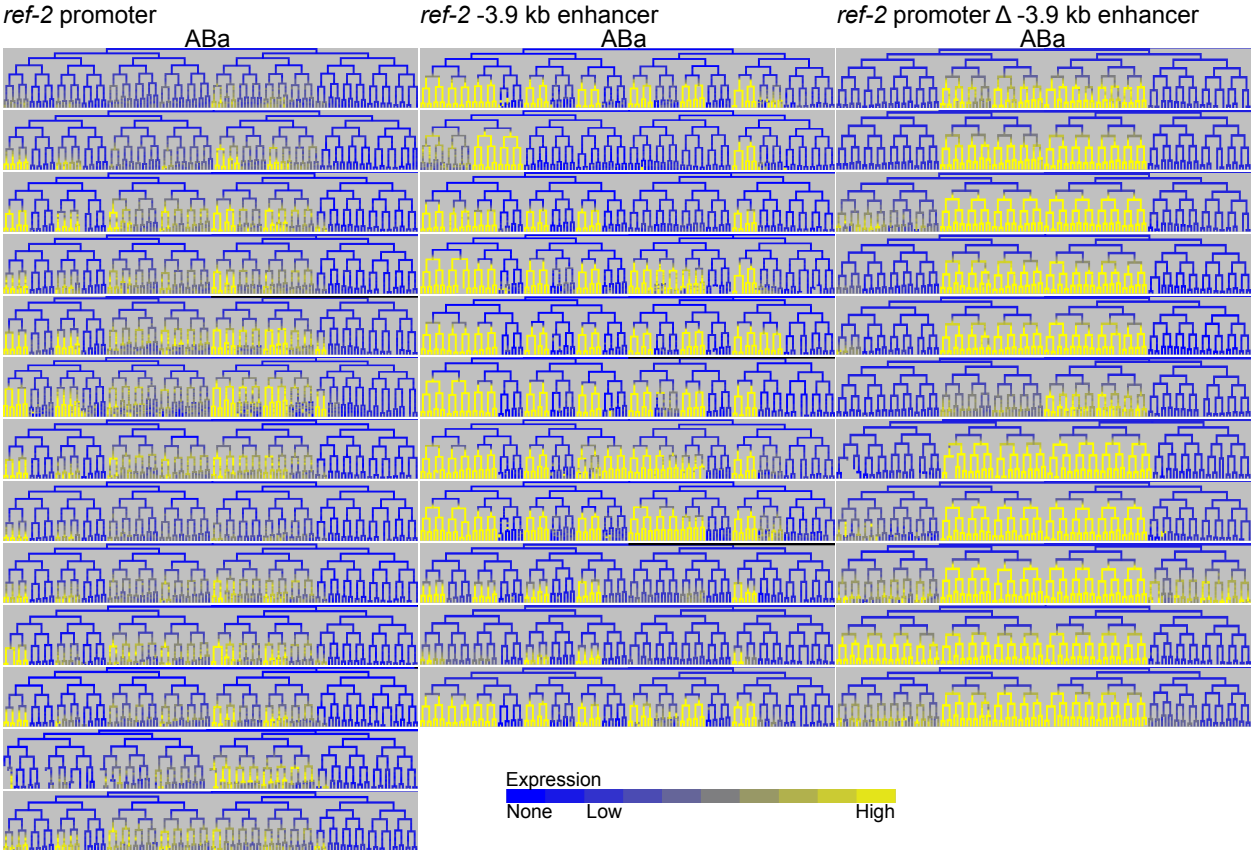

Fig S6. Expression patterns driven by the *ref-2* promoter, the -3.9 kb enhancer, and the promoter lacking the -3.9 kb enhancer are somewhat variable.
Displayed here are partial lineages for all analyzed embryos bearing these reporters to show the variation in their expression.

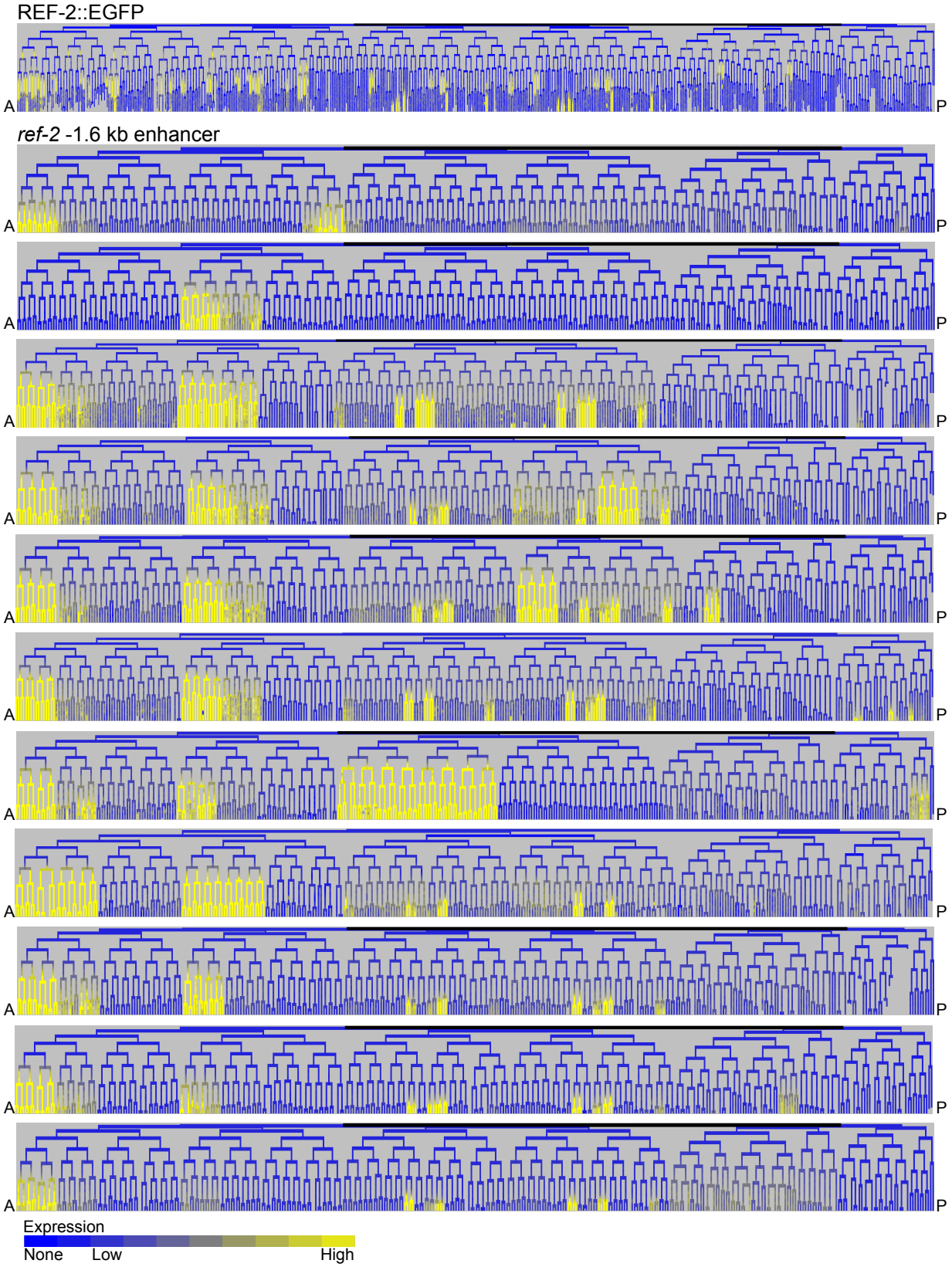
REF-2::EGFP
A
P
ref-2 -1.6 kb enhancer
A
P
A
P
A
P
A
P
A
P
A
P
A
P
A
P
A
P
A
P
A
P
Expression
None
Low
High

941 **Fig S7. Expression patterns driven by the *ref-2* -1.6 kb enhancer are variable.**
942 Displayed here are full lineages for all analyzed embryos bearing this reporter to show the variation
943 in its expression.
944

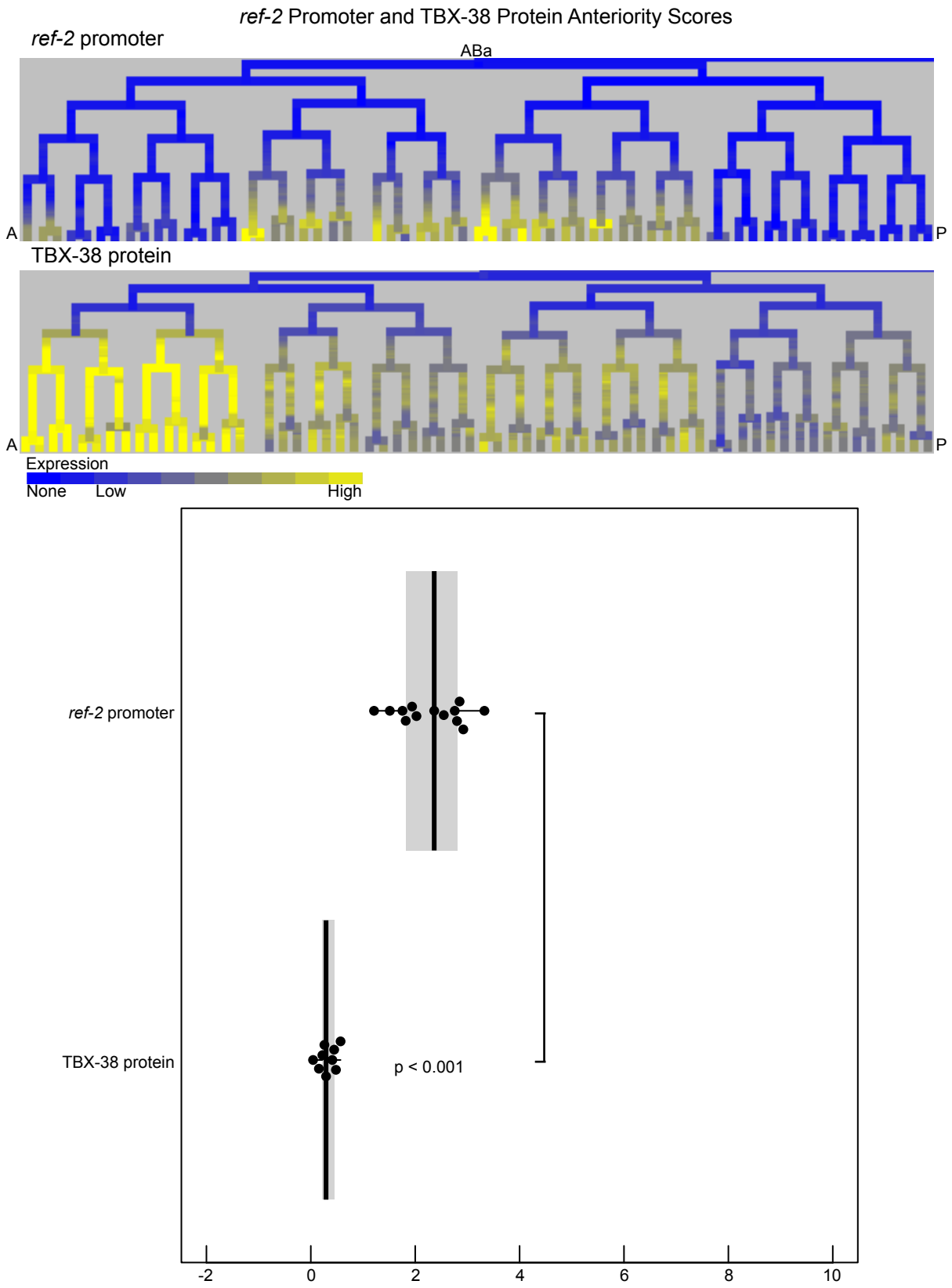
ref-2 Promoter and TBX-38 Protein Anteriority Scores
ref-2 promoter
ABa
A
P
TBX-38 protein
A
P
Expression
None
Low
High
ref-2 promoter
TBX-38 protein
p < 0.001
-2
0
2
4
6
8
10

945
946

947 **Fig S8. A TBX-38::GFP CRISPR knock-in protein reporter has minimally anterior-biased**
948 **expression in the lineages in which the *ref-2* promoter drives anterior-biased expression.**
949 Displayed are partial lineages of the P*ref-2*::*his-24*::mCherry promoter reporter expression and the
950 TBX-38::GFP CRISPR knock-in expression. The box plot shows the mean anteriority scores for
951 the *ref-2* promoter reporter and the TBX-38::GFP CRISPR knock-in for the same lineages as in
952 Fig 5J.
953

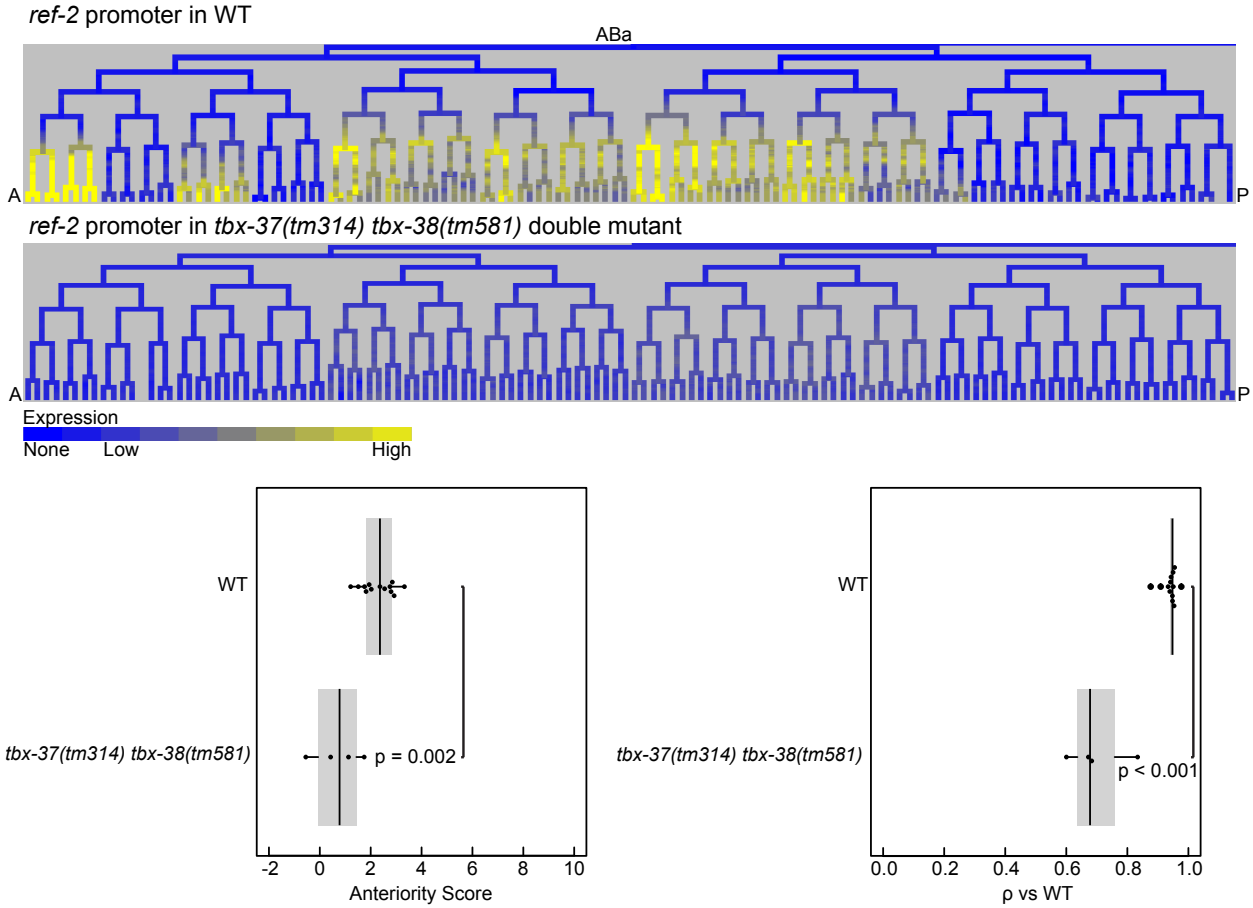

Fig S9. *tbx-37* and *tbx-38* are required for *ref-2* promoter-driven anterior-biased expression in the ABa lineage.

Displayed are partial lineages for the expression driven by the *ref-2* promoter in a WT background and in a *tbx-37(tm314) tbx-38(tm581)* double mutant background. Also shown are box plots of anteriority scores and Spearman's ρ for each of these groups, indicating a loss of anterior bias and correlation to WT for the *ref-2* promoter expression pattern in *tbx-37 tbx-38* double mutant embryos. Lineages used to determine anteriority scores are the same as in Fig 5J Spearman's ρ analysis uses the full ABa lineage expression pattern and was calculated relative to the *ref-2* promoter in the WT background.

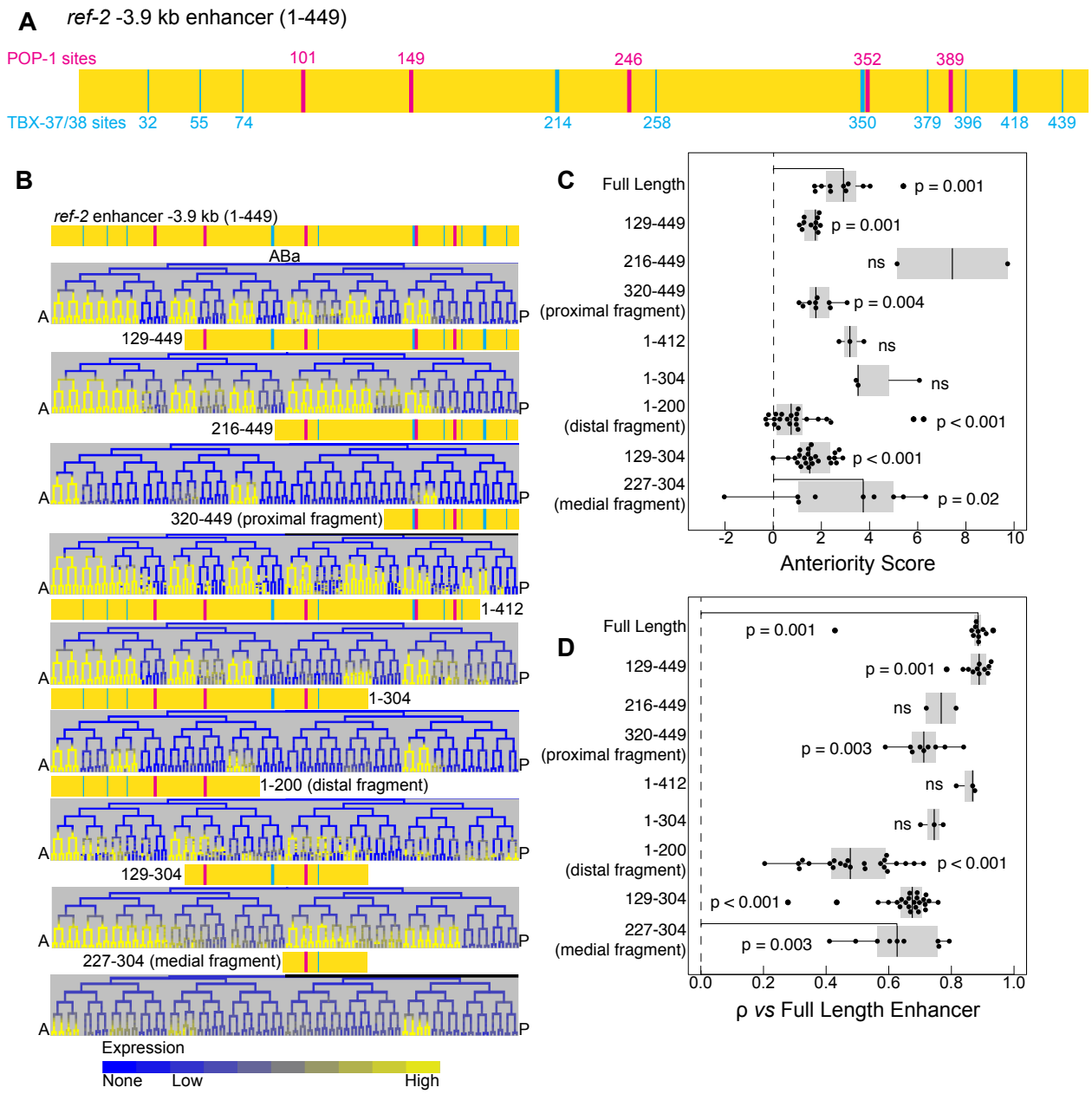

Fig S10. Three non-overlapping fragments of the -3.9 kb enhancer are each sufficient to drive anterior-biased expression in the ABa lineage of the early embryo.
(A) Model of the *ref-2* -3.9 kb enhancer with predicted TBX-37/38 and POP-1 sites indicated as in Fig 6. (B) Expression patterns driven by full-length *ref-2* -3.9 kb enhancer and by all tested fragments. (C-D) Box plots displaying the anteriority scores (C) and Spearman's ρ (D) for the full-length *ref-2* -3.9 kb enhancer and all tested fragments. Lineages used to determine anteriority scores are the same as in Fig 5J. Spearman's ρ analysis uses the full ABa lineage and was calculated relative to the full-length -3.9 kb enhancer.

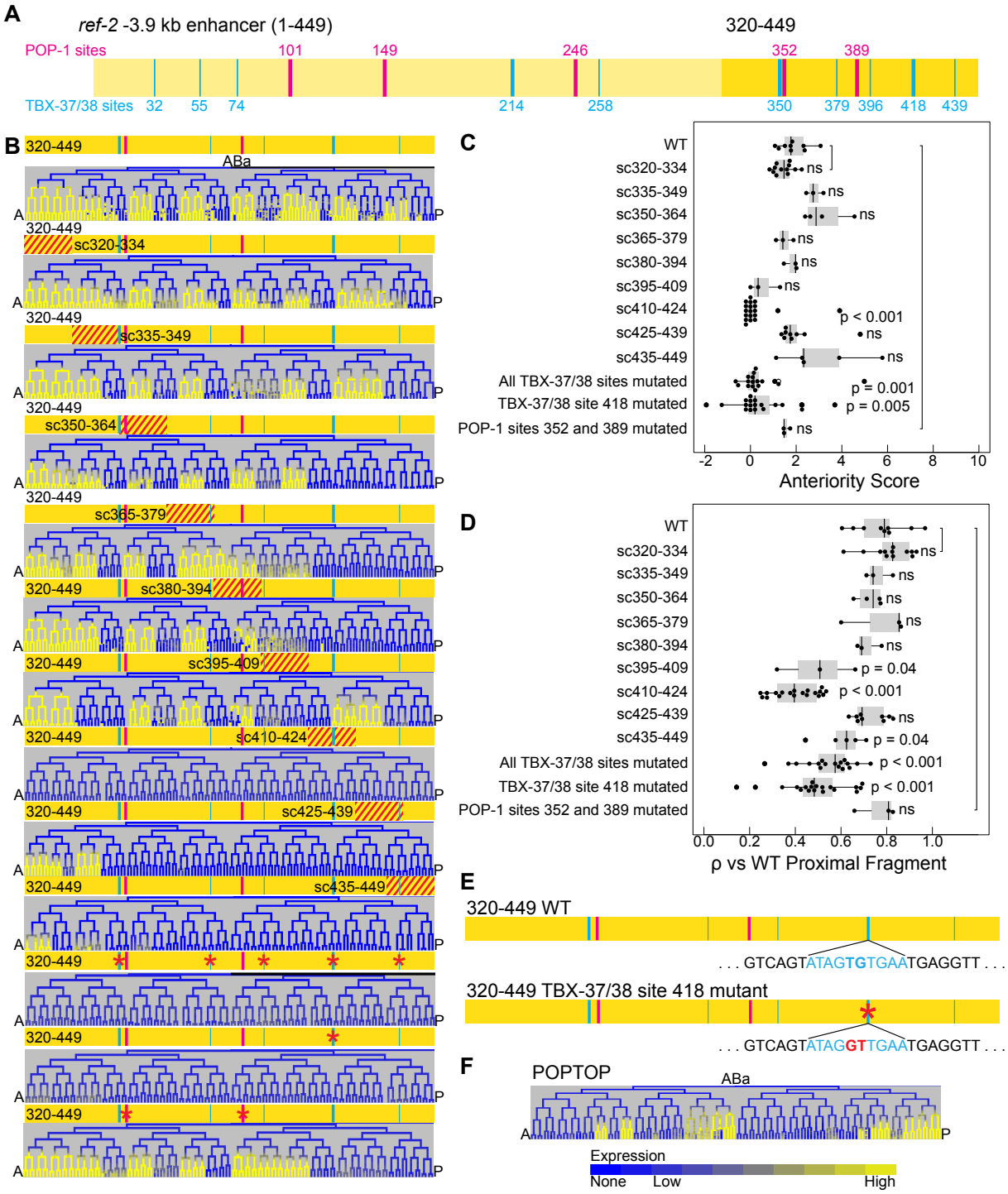

Fig S11. The broadly-expressed transcription factors *tbx-37* and *tbx-38* are required for the anterior-biased expression of *ref-2* in the ABa lineage.

(A) Model of the *ref-2* -3.9 kb enhancer with proximal fragment (base pairs 320-449) highlighted. Predicted TBX-37/38 and POP-1 sites are indicated as in Fig 6. (B) Expression patterns driven by WT proximal fragment of the *ref-2* -3.9 kb enhancer, with each 15 base-pair segment of the fragment scrambled, with all predicted TBX-37/38 sites mutated, with TBX_{418} mutated, and with

985 the two predicted POP-1 sites mutated. (C-D) Box plots displaying the anteriority scores (C) and
986 Spearman's ρ (D) for the WT proximal fragment, with each 15 base-pair segment of the fragment
987 scrambled, with all predicted TBX-37/38 sites mutated, with TBX_{418} mutated, and with the two
988 predicted POP-1 sites mutated. Lineages used to determine anteriority scores are the same as in
989 Fig 5J. Spearman's ρ analysis uses the full ABa lineage and was calculated relative to the WT
990 proximal fragment. (E) Models of the proximal fragment of the *ref-2* -3.9 kb enhancer with the
991 WT sequence of TBX_{418} and the mutated sequence used in the TBX_{418} mutant reporters. (F)
992 Expression pattern driven by the seven-copy POP-1 site concatemer POPTOP [13,51].
993

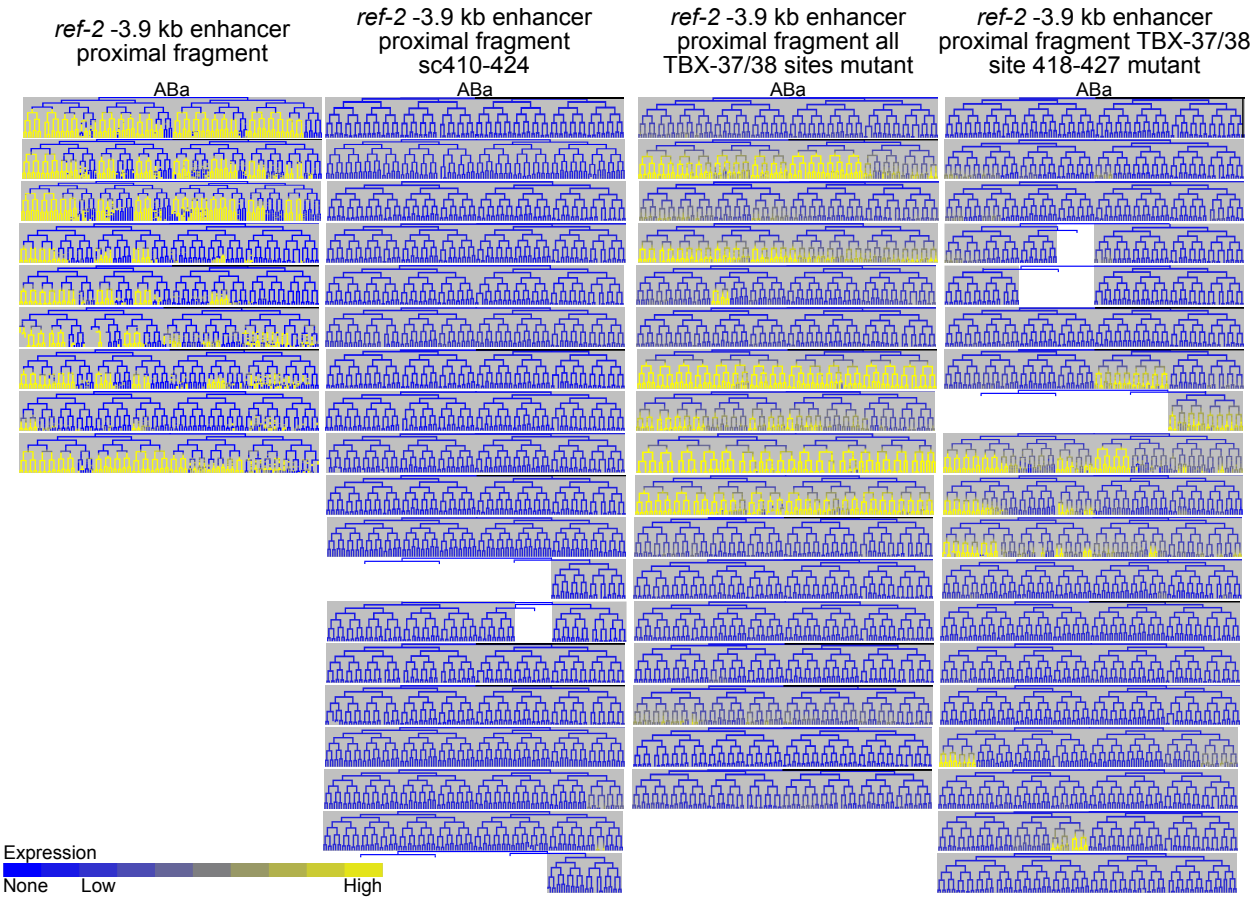

Fig S12. *ref-2* -3.9 kb enhancer WT proximal fragment, proximal fragment with all TBX-37/38 sites mutated, and proximal fragment with *TBX$_{418}$* mutated exhibit variation in their expression patterns.

Displayed are partial lineages for all analyzed embryos expressing reporters for the -3.9 kb enhancer WT proximal fragment, the *ref-2* -3.9 kb enhancer proximal fragment with base pairs 410-424 scrambled, the *ref-2* -3.9 kb enhancer proximal fragment with all TBX-37/38 sites mutated, and the *ref-2* -3.9 kb enhancer proximal fragment with *TBX$_{418}$* mutated to show the variation in the expression pattern for each of these reporters.

Table S1:
Caenorhabditis elegans strain list

Table S2:
Escherichia coli strain list

Table S3:
Quantitative analyses raw data

Table S4:
Anterior gene summary expression data

Table S5:
Recombinant DNA list

Acknowledgements:
We thank J. Archibald Millar for help with data analysis, Julia Richards for collecting and lineaging the PHA-4 movie, and Shaili Patel for her contributions as a laboratory technician. We thank Meera Sundaram for kindly permitting us to use her injection equipment. We thank Jonathan Rumley's PhD thesis committee members for helpful discussions, including committee chair Christopher Brown and committee members Michael Atchison, Peter Klein, Mary Mullins, and Meera Sundaram. Some strains were provided by the CGC, which is funded by NIH Office of Research Infrastructure Programs (P40 OD010440). We also thank the Waterston lab, the Maduro lab, and the Cochella lab for kindly providing us with *C.elegans* strains. We thank the *C. elegans* Reverse Genetics Core Facility at the University of British Columbia, which is part of the international *C. elegans* Gene Knockout Consortium, which produced the *ref-2* mutant allele (*ref-2(gk178))* used in this study. This work was funded by T32GM008216, F31GM123737, and R35GM130357.

1035 **References Cited**

1036 1. Hikasa H, Sokol SY. Wnt signaling in vertebrate axis specification. Cold Spring Harb
1037 Perspect Biol. 2013;5: a007955. doi:10.1101/cshperspect.a007955

1038 2. Archbold HC, Yang YX, Chen L, Cadigan KM. How do they do Wnt they do?: regulation
1039 of transcription by the Wnt/β-catenin pathway. Acta Physiol Oxf Engl. 2012;204: 74–109.
1040 doi:10.1111/j.1748-1716.2011.02293.x

1041 3. Martin BL, Kimelman D. Wnt signaling and the evolution of embryonic posterior
1042 development. Curr Biol CB. 2009;19: R215–R219. doi:10.1016/j.cub.2009.01.052

1043 4. Zacharias AL, Murray JI. Combinatorial decoding of the invariant C. elegans embryonic
1044 lineage in space and time. genesis. 2016;54: 182–197. doi:10.1002/dvg.22928

1045 5. Sulston JE, Schierenberg E, White JG, Thomson JN. The embryonic cell lineage of the
1046 nematode Caenorhabditis elegans. Dev Biol. 1983;100: 64–119. doi:10.1016/0012-
1047 1606(83)90201-4

1048 6. Bürglin TR, Finney M, Coulson A, Ruvkun G. Caenorhabditis elegans has scores of
1049 homoeobox-containing genes. Nature. 1989;341: 239–243. doi:10.1038/341239a0

1050 7. Chen W, Lim HH, Lim L. A new member of the ras superfamily, the rac1 homologue from
1051 Caenorhabditis elegans. Cloning and sequence analysis of cDNA, pattern of developmental
1052 expression, and biochemical characterization of the protein. J Biol Chem. 1993;268: 320–
1053 324. doi:10.1016/S0021-9258(18)54152-1

1054 8. van den Heuvel S. Cell-cycle regulation. WormBook. 2005. pp. 1–16.
1055 doi:10.1895/wormbook.1.28.1

1056 9. Shaye DD, Greenwald I. OrthoList: A Compendium of C. elegans Genes with Human
1057 Orthologs. PLOS ONE. 2011;6: e20085. doi:10.1371/journal.pone.0020085

1058 10. Kim W, Underwood RS, Greenwald I, Shaye DD. OrthoList 2: A New Comparative
1059 Genomic Analysis of Human and Caenorhabditis elegans Genes. Genetics. 2018;210: 445–
1060 461. doi:10.1534/genetics.118.301307

1061 11. Herman M. C. elegans POP-1/TCF functions in a canonical Wnt pathway that controls cell
1062 migration and in a noncanonical Wnt pathway that controls cell polarity. Development.
1063 2001;128: 581–590. doi:10.1242/dev.128.4.581

1064 12. Mizumoto K, Sawa H. Two βs or not two βs: regulation of asymmetric division by β-
1065 catenin. Trends Cell Biol. 2007;17: 465–473. doi:10.1016/j.tcb.2007.08.004

1066 13. Zacharias AL, Walton T, Preston E, Murray JI. Quantitative Differences in Nuclear β-
1067 catenin and TCF Pattern Embryonic Cells in C. elegans. Sternberg PW, editor. PLOS
1068 Genet. 2015;11: e1005585. doi:10.1371/journal.pgen.1005585

1069 14. Lin R, Hill RJ, Priess JR. POP-1 and anterior-posterior fate decisions in C. elegans
1070 embryos. Cell. 1998;92: 229–239.

1071 15. Maduro MF, Lin R, Rothman JH. Dynamics of a developmental switch: recursive
1072 intracellular and intranuclear redistribution of Caenorhabditis elegans POP-1 parallels Wnt-
1073 inhibited transcriptional repression. Dev Biol. 2002;248: 128–142.
1074 doi:10.1006/dbio.2002.0721

1075 16. Huang S, Shetty P, Robertson SM, Lin R. Binary cell fate specification during C. elegans
1076 embryogenesis driven by reiterated reciprocal asymmetry of TCF POP-1 and its
1077 coactivatorβ-catenin SYS-1. Development. 2007;134: 2685–2695. doi:10.1242/dev.008268

1078 17. Calvo D, Victor M, Gay F, Sui G, Po-Shan Luke M, Dufourcq P, et al. A POP-1 repressor
1079 complex restricts inappropriate cell type-specific gene transcription during Caenorhabditis
1080 elegans embryogenesis. EMBO J. 2001;20: 7197–7208. doi:10.1093/emboj/20.24.7197

1081 18. Maduro MF, Kasmir JJ, Zhu J, Rothman JH. The Wnt effector POP-1 and the PAL-
1082 1/Caudal homeoprotein collaborate with SKN-1 to activate C. elegans endoderm
1083 development. Dev Biol. 2005;285: 510–523. doi:10.1016/j.ydbio.2005.06.022

1084 19. Owraghi M, Broitman-Maduro G, Luu T, Roberson H, Maduro MF. Roles of the Wnt
1085 effector POP-1/TCF in the C. elegans endomesoderm specification gene network. Dev Biol.
1086 2010;340: 209–221. doi:10.1016/j.ydbio.2009.09.042

1087 20. Murgan S, Kari W, Rothbächer U, Iché-Torres M, Mélénec P, Hobert O, et al. Atypical
1088 Transcriptional Activation by TCF via a Zic Transcription Factor in C. elegans Neuronal
1089 Precursors. Dev Cell. 2015;33: 737–745. doi:10.1016/j.devcel.2015.04.018

1090 21. Murgan S, Bertrand V. How targets select activation or repression in response to Wnt.
1091 Worm. 2015;4: e1086869. doi:10.1080/21624054.2015.1086869

1092 22. Zhang CU, Blauwkamp TA, Burby PE, Cadigan KM. Wnt-Mediated Repression via
1093 Bipartite DNA Recognition by TCF in the Drosophila Hematopoietic System. Desplan C,
1094 editor. PLoS Genet. 2014;10: e1004509. doi:10.1371/journal.pgen.1004509

1095 23. Sulston JE, Horvitz HR. Post-embryonic cell lineages of the nematode, Caenorhabditis
1096 elegans. Dev Biol. 1977;56: 110–156. doi:10.1016/0012-1606(77)90158-0

1097 24. Murray JI, Boyle TJ, Preston E, Vafeados D, Mericle B, Weisdepp P, et al.
1098 Multidimensional regulation of gene expression in the C. elegans embryo. Genome Res.
1099 2012;22: 1282–1294. doi:10.1101/gr.131920.111

1100 25. Ma X, Zhao Z, Xiao L, Xu W, Kou Y, Zhang Y, et al. A 4D single-cell protein atlas of
1101 transcription factors delineates spatiotemporal patterning during embryogenesis. Nat
1102 Methods. 2021;18: 893–902. doi:10.1038/s41592-021-01216-1

1103 26. Murray JI, Bao Z, Boyle TJ, Boeck ME, Mericle BL, Nicholas TJ, et al. Automated
1104 analysis of embryonic gene expression with cellular resolution in C. elegans. Nat Methods.

1105 2008;5: 703–709. doi:10.1038/nmeth.1228

1106 27. Packer Jonathan S., Zhu Qin, Huynh Chau, Sivaramakrishnan Priya, Preston Elicia, Dueck
1107 Hannah, et al. A lineage-resolved molecular atlas of C. elegans embryogenesis at single-cell
1108 resolution. Science. 2019;365: eaax1971. doi:10.1126/science.aax1971

1109 28. Bao Z, Murray JI, Boyle T, Ooi SL, Sandel MJ, Waterston RH. Automated cell lineage
1110 tracing in Caenorhabditis elegans. Proc Natl Acad Sci U S A. 2006;103: 2707.
1111 doi:10.1073/pnas.0511111103

1112 29. Santella A, Du Z, Nowotschin S, Hadjantonakis A-K, Bao Z. A hybrid blob-slice model for
1113 accurate and efficient detection of fluorescence labeled nuclei in 3D. BMC Bioinformatics.
1114 2010;11: 580. doi:10.1186/1471-2105-11-580

1115 30. Boyle TJ, Bao Z, Murray JI, Araya CL, Waterston RH. AceTree: a tool for visual analysis
1116 of Caenorhabditis elegans embryogenesis. BMC Bioinformatics. 2006;7: 275.
1117 doi:10.1186/1471-2105-7-275

1118 31. Katzman B, Tang D, Santella A, Bao Z. AceTree: a major update and case study in the long
1119 term maintenance of open-source scientific software. BMC Bioinformatics. 2018;19: 121.
1120 doi:10.1186/s12859-018-2127-0

1121 32. Yanai I, Baugh LR, Smith JJ, Roehrig C, Shen-Orr SS, Claggett JM, et al. Pairing of
1122 competitive and topologically distinct regulatory modules enhances patterned gene
1123 expression. Mol Syst Biol. 2008;4. doi:10.1038/msb.2008.6

1124 33. Lin R, Thompson S, Priess JR. pop-1 encodes an HMG box protein required for the
1125 specification of a mesoderm precursor in early C. elegans embryos. Cell. 1995;83: 599–
1126 609. doi:10.1016/0092-8674(95)90100-0

1127 34. Kidd AR, Miskowski JA, Siegfried KR, Sawa H, Kimble J. A β-Catenin Identified by
1128 Functional Rather Than Sequence Criteria and Its Role in Wnt/MAPK Signaling. Cell.
1129 2005;121: 761–772. doi:10.1016/j.cell.2005.03.029

1130 35. Phillips BT, Kidd AR, King R, Hardin J, Kimble J. Reciprocal asymmetry of SYS-1/beta-
1131 catenin and POP-1/TCF controls asymmetric divisions in Caenorhabditis elegans. Proc Natl
1132 Acad Sci. 2007;104: 3231–3236. doi:10.1073/pnas.0611507104

1133 36. Broitman-Maduro G, Owraghi M, Hung WWK, Kuntz S, Sternberg PW, Maduro MF. The
1134 NK-2 class homeodomain factor CEH-51 and the T-box factor TBX-35 have overlapping
1135 function in C. elegans mesoderm development. Dev Camb Engl. 2009;136: 2735–2746.
1136 doi:10.1242/dev.038307

1137 37. Broitman-Maduro G, Lin KT-H, Hung WWK, Maduro MF. Specification of the C. elegans
1138 MS blastomere by the T-box factor TBX-35. Dev Camb Engl. 2006;133: 3097–3106.
1139 doi:10.1242/dev.02475

1140 38. Alper S, Kenyon C. The zinc finger protein REF-2 functions with the Hox genes to inhibit

1141 cell fusion in the ventral epidermis of C. elegans. Development. 2002;129: 3335–3348.
1142 doi:10.1242/dev.129.14.3335

1143 39. Walton T, Preston E, Nair G, Zacharias AL, Raj A, Murray JI. The Bicoid Class
1144 Homeodomain Factors ceh-36/OTX and unc-30/PITX Cooperate in C. elegans Embryonic
1145 Progenitor Cells to Regulate Robust Development. PLOS Genet. 2015;11: e1005003.
1146 doi:10.1371/journal.pgen.1005003

1147 40. Richards JL, Zacharias AL, Walton T, Burdick JT, Murray JI. A quantitative model of
1148 normal Caenorhabditis elegans embryogenesis and its disruption after stress. Dev Biol.
1149 2013;374: 12–23. doi:10.1016/j.ydbio.2012.11.034

1150 41. Maduro MF, Meneghini MD, Bowerman B, Broitman-Maduro G, Rothman JH. Restriction
1151 of Mesendoderm to a Single Blastomere by the Combined Action of SKN-1 and a GSK-3β
1152 Homolog Is Mediated by MED-1 and -2 in C. elegans. Mol Cell. 2001;7: 475–485.
1153 doi:10.1016/S1097-2765(01)00195-2

1154 42. Maduro MF, Hill RJ, Heid PJ, Newman-Smith ED, Zhu J, Priess JR, et al. Genetic
1155 redundancy in endoderm specification within the genus Caenorhabditis. Dev Biol.
1156 2005;284: 509–522. doi:10.1016/j.ydbio.2005.05.016

1157 43. Boeck ME, Boyle T, Bao Z, Murray J, Mericle B, Waterston R. Specific roles for the
1158 GATA transcription factors end-1 and end-3 during C. elegans E-lineage development.
1159 Spec Sect Hist Dev Biol. 2011;358: 345–355. doi:10.1016/j.ydbio.2011.08.002

1160 44. Good K, Ciosk R, Nance J, Neves A, Hill RJ, Priess JR. The T-box transcription factors
1161 TBX-37 and TBX-38 link GLP-1/Notch signaling to mesoderm induction in C. elegans
1162 embryos. Development. 2004;131: 1967–1978. doi:10.1242/dev.01088

1163 45. Andachi Y. Caenorhabditis elegans T-box genes tbx-9 and tbx-8 are required for formation
1164 of hypodermis and body-wall muscle in embryogenesis. Genes Cells. 2004;9: 331–344.
1165 doi:10.1111/j.1356-9597.2004.00725.x

1166 46. Neves A, Priess JR. The REF-1 Family of bHLH Transcription Factors Pattern C. elegans
1167 Embryos through Notch-Dependent and Notch-Independent Pathways. Dev Cell. 2005;8:
1168 867–879. doi:10.1016/j.devcel.2005.03.012

1169 47. Siepel A, Bejerano G, Pedersen JS, Hinrichs AS, Hou M, Rosenbloom K, et al.
1170 Evolutionarily conserved elements in vertebrate, insect, worm, and yeast genomes. Genome
1171 Res. 2005;15: 1034–1050. doi:10.1101/gr.3715005

1172 48. Pollard KS, Hubisz MJ, Rosenbloom KR, Siepel A. Detection of nonneutral substitution
1173 rates on mammalian phylogenies. Genome Res. 2010;20: 110–121.
1174 doi:10.1101/gr.097857.109

1175 49. Kent WJ, Sugnet CW, Furey TS, Roskin KM, Pringle TH, Zahler AM, et al. The Human
1176 Genome Browser at UCSC. Genome Res. 2002;12: 996–1006. doi:10.1101/gr.229102

1177 50. Charest J, Daniele T, Wang J, Bykov A, Mandlbauer A, Asparuhova M, et al.
1178 Combinatorial Action of Temporally Segregated Transcription Factors. Dev Cell. 2020;55:
1179 483-499.e7. doi:10.1016/j.devcel.2020.09.002

1180 51. LaBonty M, Szmygiel C, Byrnes LE, Hughes S, Woollard A, Cram EJ. CACN-1/Cactin
1181 plays a role in Wnt signaling in C. elegans. PloS One. 2014;9.
1182 doi:10.1371/journal.pone.0101945

1183 52. Murray JI, Preston E, Crawford JP, Rumley JD, Amom P, Anderson BD, et al. The anterior
1184 Hox gene ceh-13 and elt-1/GATA activate the posterior Hox genes
1185 nob-1 and php-3 to specify posterior lineages in the C.
1186 elegans embryo. bioRxiv. 2021; 2021.02.09.430385. doi:10.1101/2021.02.09.430385

1187 53. Poole RJ, Hobert O. Early Embryonic Programming of Neuronal Left/Right Asymmetry in
1188 C. elegans. Curr Biol. 2006;16: 2279–2292. doi:10.1016/j.cub.2006.09.041

1189 54. Fukushige T, Brodigan TM, Schriefer LA, Waterston RH, Krause M. Defining the
1190 transcriptional redundancy of early bodywall muscle development in C. elegans: evidence
1191 for a unified theory of animal muscle development. Genes Dev. 2006;20: 3395–3406.
1192 doi:10.1101/gad.1481706

1193 55. Fukushige T, Krause M. The myogenic potency of HLH-1 reveals wide-spread
1194 developmental plasticity in early C. elegans embryos. Dev Camb Engl. 2005;132: 1795–
1195 1805. doi:10.1242/dev.01774

1196 56. Simonis N, Rual J-F, Carvunis A-R, Tasan M, Lemmens I, Hirozane-Kishikawa T, et al.
1197 Empirically controlled mapping of the Caenorhabditis elegans protein-protein interactome
1198 network. Nat Methods. 2009;6.

1199 57. Tintori SC, Osborne Nishimura E, Golden P, Lieb JD, Goldstein B. A Transcriptional
1200 Lineage of the Early C. elegans Embryo. Dev Cell. 2016;38: 430–444.
1201 doi:10.1016/j.devcel.2016.07.025

1202 58. Whiting J, Marshall H, Cook M, Krumlauf R, Rigby PW, Stott D, et al. Multiple spatially
1203 specific enhancers are required to reconstruct the pattern of Hox-2.6 gene expression.
1204 Genes Dev. 1991;5: 2048–2059. doi:10.1101/gad.5.11.2048

1205 59. Epstein DJ, McMahon AP, Joyner AL. Regionalization of Sonic hedgehog transcription
1206 along the anteroposterior axis of the mouse central nervous system is regulated by Hnf3-
1207 dependent and -independent mechanisms. Development. 1999;126: 281–292.
1208 doi:10.1242/dev.126.2.281

1209 60. Teng Y, Girard L, Ferreira HB, Sternberg PW, Emmons SW. Dissection of cis-regulatory
1210 elements in the C. elegans Hox gene egl-5 promoter. Dev Biol. 2004;276: 476–492.
1211 doi:10.1016/j.ydbio.2004.09.012

1212 61. Streit A, Kohler R, Marty T, Belfiore M, Takacs-Vellai K, Vigano M-A, et al. Conserved
1213 Regulation of the Caenorhabditis elegans labial/Hox1 Gene ceh-13. Dev Biol. 2002;242:

1214 96–108. doi:10.1006/dbio.2001.0544

1215 62. Landmann F, Quintin S, Labouesse M. Multiple regulatory elements with spatially and
1216 temporally distinct activities control the expression of the epithelial differentiation gene lin-
1217 26 in C. elegans. Dev Biol. 2004;265: 478–490. doi:10.1016/j.ydbio.2003.09.009

1218 63. Chen RA-J, Down TA, Stempor P, Chen QB, Egelhofer TA, Hillier LW, et al. The
1219 landscape of RNA polymerase II transcription initiation in C. elegans reveals promoter and
1220 enhancer architectures. Genome Res. 2013;23: 1339–1347. doi:10.1101/gr.153668.112

1221 64. Serizay J, Dong Y, Jänes J, Chesney M, Cerrato C, Ahringer J. Distinctive regulatory
1222 architectures of germline-active and somatic genes in C. elegans. Genome Res. 2020;30:
1223 1752–1765. doi:10.1101/gr.265934.120

1224 65. Bertrand V, Hobert O. Linking asymmetric cell division to the terminal differentiation
1225 program of postmitotic neurons in C. elegans. Dev Cell. 2009;16: 563–575.
1226 doi:10.1016/j.devcel.2009.02.011

1227 66. Kuersten S, Segal SP, Verheyden J, LaMartina SM, Goodwin EB. NXF-2, REF-1, and
1228 REF-2 Affect the Choice of Nuclear Export Pathway for tra-2 mRNA in C. elegans. Mol
1229 Cell. 2004;14: 599–610. doi:10.1016/j.molcel.2004.05.004

1230 67. Clark E, Akam M. Odd-paired controls frequency doubling in Drosophila segmentation by
1231 altering the pair-rule gene regulatory network. Wittkopp PJ, editor. eLife. 2016;5: e18215.
1232 doi:10.7554/eLife.18215

1233 68. Yoon Y, Klomp J, Martin-Martin I, Criscione F, Calvo E, Ribeiro J, et al. Embryo polarity
1234 in moth flies and mosquitoes relies on distinct old genes with localized transcript isoforms.
1235 Wittkopp PJ, Pick L, Popadic A, Akam M, editors. eLife. 2019;8: e46711.
1236 doi:10.7554/eLife.46711

1237 69. Kamath RS, Fraser AG, Dong Y, Poulin G, Durbin R, Gotta M, et al. Systematic functional
1238 analysis of the Caenorhabditis elegans genome using RNAi. Nature. 2003;421: 231–237.
1239 doi:10.1038/nature01278

1240 70. Vora S, Phillips BT. Centrosome-Associated Degradation Limits β-Catenin Inheritance by
1241 Daughter Cells after Asymmetric Division. Curr Biol. 2015;25: 1005–1016.
1242 doi:10.1016/j.cub.2015.02.020

1243 71. Weirauch MT, Yang A, Albu M, Cote AG, Montenegro-Montero A, Drewe P, et al.
1244 Determination and inference of eukaryotic transcription factor sequence specificity. Cell.
1245 2014;158: 1431–1443. doi:10.1016/j.cell.2014.08.009

1246 72. Narasimhan K, Lambert SA, Yang AWH, Riddell J, Mnaimneh S, Zheng H, et al. Mapping
1247 and analysis of transcription factor sequence specificities. eLife. 2015;4.
1248 doi:10.7554/eLife.06967

1249 73. Bao Z, Murray JI. Mounting Caenorhabditis elegans Embryos for Live Imaging of

1250 Embryogenesis. Cold Spring Harb Protoc. 2011;2011: pdb.prot065599.
1251 doi:10.1101/pdb.prot065599